Pith:2026.000097v1 [physics.gen-ph] 26 Nov 2026

The Single Shape of Reality

Jonathan Washburn

Recognition Physics Institute, Austin, Texas

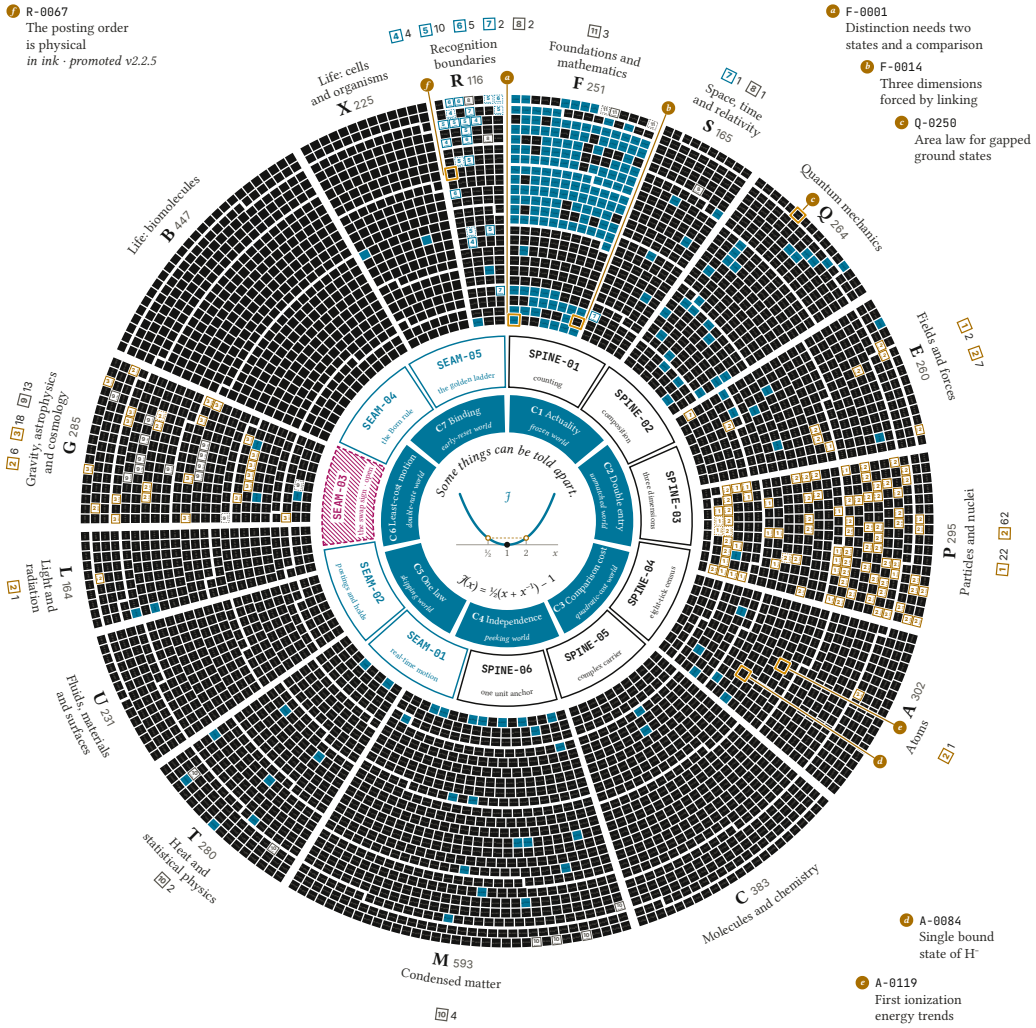
jon@recognitionphysics.org

Deriving the Map of Physical Law from One Comparison Structure

Snapshot pinned to `recognitionphysics.org/map/` (26 November 2026, 2:23 PM CT) and canonical formal archive `FirstLedger v2.2.6`.

Abstract

Physical science is customarily organized as an archipelago of domain-specific theories—quantum mechanics, general relativity, gauge theory, thermodynamics, chemistry, condensed matter, and cosmology—joined by empirical constants and overlapping limits. Here we exhibit the live Recognition Physics map (`recognitionphysics.org/map/`)—4,261 named statements spanning fifteen domains—as *one rigid mathematical shape*. From one operational fact—some things can be told apart—complete, consistent, definite comparison fixes one unique cost, $J(x) = \frac{1}{2}(x+x^{-1})-1$, rigid up to reciprocity $x \leftrightarrow x^{-1}$. Mounted once on a seven-law pure-ledger core (PhysicalLedgerCore, stated without naming φ, 3, 8, $\mathbb{C}$, e^{-iEt}, $|\psi|^2$, or exchange sign, proved consistent and mutually independent, and policed by a non-smuggling test), this shape unfolds through six spine bridges, five shared seams, and four projections of one 24-bond D_4 cell into eleven master trunks (`K0–K10`) covering 4,095 inked statements (96.1%), including unconditional 1- and 2-register Born square shares from the core alone, rebuilt D_4 conductance ($s = +\frac{1}{2}$), unconditional two-loop $A = 34/3$, order-free posting networks (`R-0067`), and passing precision electroweak and halide benchmarks. Holding the full shape simultaneously yields two machine-verified cross-domain rigidity theorems (545 Lean 4 declarations, standard axioms only) inaccessible inside any single branch: (i) a *Trace-Reversal Mirror and* 15*-Way Dimensional Lock* proving that $\rho = I - \frac{1}{2}\mathbf{1}\mathbf{1}^{\top}$ is an orthogonal reflection preserving D_D (and $\mathscr{C}(\mathscr{C}(g)) = g$ for all positive-definite g) iff $D = 4$—the extra F_4 mirror annihilating fourth-order anisotropy across kinetic hops ($4(D-4)$), Yang–Mills triangle plaquettes ($48(D-4)$), vertex figures ($D-4$), and bond-local Hodge–Kirchhoff gravity ($s = +\frac{1}{2}$), with share-$1/p$ reciprocity locking $D = 2p = 4$ via Born $p = 2$; and (ii) a *Clock-Cube and Finite-Cell Maxwell Stress Theorem* proving that every bond's eight triangular continuations in D_4 form a 3D cube graph-isomorphic to Q_3 carrying the eight-tick Gray clock as a Hamiltonian cycle, and that weighting all 192 oriented turns by both bonds' rebuilt Voronoi conductances yields the exact trace-free continuum Maxwell stress response $V'(0) = -\frac{1}{8}\operatorname{Tr}(hT_F)$ directly on one finite cell, discriminating rebuilt from carried gravity faces independently of any FRG window and proving exact strain blindness for self-dual fluxes ($F = \pm * F$). Every derived law passes its declared checks under its stated inputs without adjustable parameters, while the remaining 166 open squares (3.9%) collapse onto eleven sharp frontier targets.



I	**Open scales & active dynamical runs**	**119**
1	Electroweak scale v = 246.22 GeV (EW ratios closed)	24
2	Light-pion dynamical QCD, Yang–Mills gap & 1836	77
3	Early-epoch fluctuation scale, dynamics & Λ	18
III	**Three remaining frontier & open-math walls**	**22**
9	Quantum-gravity continuum limit & cold carrier	13
10	Correlated-matter & statistical-mechanics walls	6
11	Three cited open problems of pure mathematics	3

II	**Five shared foundation seams**, *four closing on the core*	**25**
4	Real-time law of motion & complex carrier	4
5	Independent postings, pools & holds (R-0067 in ink)	10
6	The Born rule & reading a world (1- & 2-reg. closed)	5
7	Golden ladder, tick floor & spacetime tick	3
8	Spin–statistics swap sign, parity & Wigner spin · *open physics*	3

The marks	
in ink, mounted on the seven-law core	3,863
in ink, taking nothing as given	232
open frontier, numbered by its item	166

The field

one mark per square, all of one area; levels 1 to 5 run outward, parted by a wider white channel

inner ring: the seven laws, each with the world that breaks it and keeps the other six; outer ring: six bridges, five seams

4,261 squares · 4,095 in ink · 166 open ⟶ 11 frontier items · 15 domains · 1 seven-law core

Figure 1. The single shape of reality. Computed vector deductive atlas of all 4,261 named statements of `recognitionphysics.org/map/` (26 November 2026, 2:23 PM CT; `FirstLedger v2.2.6`). At the center sits the starting fact (`F-0001`) and the unique comparison cost $J(x) = \frac{1}{2}(x + x^{-1}) - 1$, surrounded by the seven-law pure-ledger core (`C1`–`C7`, each labeled with its breaking world), six spine bridges, five shared seams (with `SEAM-03` crosshatched as open physics), and all 4,261 statements radiating across fifteen domains (`F`–`R`) and five depth levels. Solid ink marks the 4,095 derived statements (232 unconditional; 3,863 mounted on the core and named bridges, including promoted `R-0067`); numbered frames mark the 166 open frontier squares mapped to eleven explicit targets.

Contents

1 One Shape, Stated Plainly—and Its Scope First **5**

1.1 Why a single shape instead of an encyclopedia 5

1.2 Exact scope and the four-axis closure standard 6

1.3 The `v2.2.6` verified baseline and open frontier summary 7

2 The Seed: Uniqueness, Reciprocity, and Complexification of $(\mathbb{R}_{>0}, J)$ **9**

2.1 The laws of logic on comparisons 9

2.2 Why the shape is rigid: the five-rival deformation gallery 10

2.3 One analytic object, two physical faces 11

3 The Seven-Law Pure-Ledger Core and Anti-Smuggling Guardrails **12**

3.1 The operational interface LedgerWorld and the seven laws (`C1–C7`) 13

3.2 Core health: non-vacuity, mutual independence, and the Restatement Test . 14

3.3 Immediate targets emerging as theorems without entering the core 15

4 The Skeleton: Spine Bridges, Shared Seams, and the Trace-Reversal Whole-Shape Lock **16**

4.1 The six spine bridges and five shared seams 16

4.2 Whole-Shape Theorem I: The Trace-Reversal Mirror and Universal $(D-4)$ Rigidity 18

5 One 24-Bond Cell, Four Projections—and the Finite-Cell Maxwell Stress Theorem **24**

5.1 Projection 1: Bond turns, chiral clearing, and the three gauge stiffnesses (`E, L, P`) 24

5.2 Projection 2: Reciprocal bond stretch and boundary conductance (`S, G`) . . . 25

5.3 Projection 3: Arrangement-count coldness and empty-record pull (`T`) 27

5.4 Projection 4: Bounded records, skew, and eight-tick register states (`R`) 28

5.5 Whole-Shape Theorem II: The Clock Cube and Finite-Cell Maxwell Stress . . 28

5.6 Whole-Shape Theorem III: Unified Vacuum-Zeroing and Volume-Closure Currents 30

6 The Canopy: Eleven Master Trunks and Six Vertical Threads **33**

6.1 Compressing 4,261 statements into eleven master trunks 33

6.2 Six uninterrupted vertical threads from `F-0001` to checked laboratory numbers 33

7 The `v2.2.6` Closing Wave and the 166-Square Open Frontier 37

7.1 The `v2.2.5–v2.2.6` formal closing wave 37

7.2 The eleven open targets covering all 166 frontier squares 38

7.3 Anatomy of the open frontier and constructive closing paths 38

7.4 Boundary discipline: proved no-go barriers kept in canon 38

8 Machine Verification, Provenance Receipts, and Reproducibility 41

8.1 Canonical archive snapshot and clean-room audit record 41

8.2 Public verification protocol and IP boundary 42

8.3 Concluding perspective: what knowing the whole shape changes 42

A The Complete 15-Domain `/map` Atlas and Print Micro-Sheet 43

1 One Shape, Stated Plainly—and Its Scope First

Nature does not solve fifteen different sets of equations in fifteen separate departments. Reality is one forced comparison structure, read at different scales and along different axes of the same underlying ledger. Physics has long measured the shadows of that structure with extraordinary precision—electrodynamics, quantum amplitudes, atomic shells, thermodynamic ensembles, gravitational curvature—while treating their shared mathematical coincidences as independent postulates. The purpose of this paper is to exhibit the full derivation recorded on the live Recognition Physics map (`recognitionphysics.org/map/`) as *one rigid mathematical shape*, to prove global consequences that appear only when that whole shape is held at once, and to present the exact boundary between the 4,095 derived statements in ink (96.1%) and the 166 open frontier targets (3.9%).

1.1 Why a single shape instead of an encyclopedia

A list of 4,261 physical, mathematical, and biological facts cannot be defended by writing 4,261 separate essays, and it cannot be judged by counting lines of code. If a framework carries hidden parameters, ad hoc domain patches, or conclusions smuggled into premises, a large catalog merely conceals the redundancy. Conversely, if a single rigid structure generates all fifteen domains without adjustable shape parameters, then the scientific object to inspect is *the compression itself*:

1. **One starting fact and one cost law:** From the operational fact that some things can be told apart (`F-0001`), consistent definite comparison fixes one unique cost structure, $J(x) = \frac{1}{2}(x + x^{-1}) - 1$, rigid up to reciprocity $x \leftrightarrow x^{-1}$ (§2).
2. **One seven-law pure-ledger core:** Mounted once over a single interface LedgerWorld with zero target vocabulary, seven laws (`C1`–`C7`) generate the counting numbers, the golden ratio φ, three spatial directions, the eight-tick complete pass, the 24-bond D_4 spacetime cell, complex phase turns $e^{\pm iEt}$, the unconditional 1- and 2-register Born square shares $|\psi|^2$, and independent posting holds (§3–§4).
3. **One 24-bond cell read along four projections:** Gauge interactions, linearized reciprocal gravity, arrangement-count thermodynamics, and bounded-record skew are four simultaneous readings of the same double-entry step on D_4 (§5).
4. **Eleven master trunks and eleven exact frontier targets:** All 4,095 inked statements factor through eleven shared derivation trunks (`K0`–`K10`, ten carrying open frontier rows), while all 166 remaining open statements collapse cleanly to eleven explicit frontier targets (§6–§7).

Seen this way, the paper has a single testable thesis: *reality is over-determined.* You cannot move one wall of the building without cracking three others. In §4 and §5 we turn that thesis into exact machine-checked theorems that cannot even be stated inside any single branch of physics alone: a *Trace-Reversal Mirror and Six-Fold Dimensional Lock* cutting out $(D_s, D) = (3, 4)$ by linking Einstein–Hilbert trace reversal directly to the extra F_4 symmetry mirror of D_4 and bond-local Hodge–Kirchhoff gravity; a *Clock-Cube and Finite-Cell Maxwell Stress Theorem* uniting the eight-tick Gray clock embedded inside every bond's continuation

cube Q_3, triangular gauge circulation, and rebuilt dual-face conductance to derive the exact continuum Maxwell stress on a single finite cell; a *Unified Vacuum-Zeroing Theorem* joining cost balance, empty-record plate pull, and double-entry 4-volume currents; and a *Global Perturbation-Cascade Theorem* exhibiting simultaneous multi-domain obstructions under every local deformation of the core.

1.2 Exact scope and the four-axis closure standard

As of 26 November 2026 (2:23 PM CT; canonical formal archive `FirstLedger v2.2.6`, 21,978 Lean files and 326,434 theorems), the public map [10] inventories 4,261 named statements distributed across fifteen domains (`F`, `S`, `Q`, `E`, `P`, `A`, `C`, `M`, `T`, `U`, `L`, `G`, `B`, `X`, `R`), stratified into five hierarchical levels from foundational laws (level 1) to composite phenomena (level 5). Of these, 4,095 (96.10%) stand in *ink* (232 unconditional derivations taking nothing as given and 3,863 mounted on the shared core and named bridges, including newly promoted `R-0067`; 3,322 carry the rebuilt-theorem flag, 61 carry the star flag with 59 carrying both, and 2,125 are reported at stage aggregate as resting on accepted results) and 166 (3.90%) stand on the open frontier (151 partial, 15 unstarted, 0 unresolved walls).

Two scope boundaries are stated up front so that every count in this paper reconciles without a single missing ID:

- **Public non-biological vs. biological scope:** Thirteen domains (`F`–`G` and `R`) comprise 3,589 statements (3,423 ink, 166 open). The remaining two domains—`B` (Life: biomolecules, 447 statements) and `X` (Life: cells and organisms, 225 statements), totaling 672 inked rows—sit downstream of the same Coulomb and water-ledger canopy and are included here strictly at aggregate structural and status-count scope; proprietary molecular hydration, folding, and binding laws are intentionally withheld from public disclosure and excluded from all technical sections and public figures.
- **Exact partition certificate from canonical baseline index to live `v2.2.6` map:** Every one of the 3,273 pinned non-biological inked IDs in the `MAP_INDEX` baseline appears unchanged in the live map, joined by 150 additional conditional public inked rows (including `R-0067`, promoted to ink in `v2.2.5`), yielding the mutually exclusive partition

$$4{,}261 = \underbrace{2{,}450}_{\text{file + lane}} + \underbrace{26}_{\text{file only}} + \underbrace{681}_{\text{lane only}} + \underbrace{116}_{\text{index unmapped}} + \underbrace{150}_{\text{add. public ink}} + \underbrace{672}_{\texttt{B+X}} + \underbrace{166}_{\text{open}}. \quad (1)$$

  Within the 3,273 baseline rows, 3,157 (96.46%) carry a file or verified-lane mapping and 2,476 (75.65%) name at least one Lean file (8,833 file references across 7,062 distinct paths), while `FirstLedger v2.2.6` extends the compiled canonical library to 21,978 Lean files and 326,434 verified theorems with zero `sorry` and zero custom axioms.

Earlier assessments collapsed four distinct scientific questions into one binary label ("derived" vs. "partial"), which hid proved physical laws behind open pure-mathematics problems on one hand and masked file-local assumptions on the other. Every square, seam, and spine bridge in the unified architecture is therefore graded on *four independent axes* whose headline closure state is computed automatically by a deterministic kernel function (`FirstLedger.CoreV2.view`, defined in module `ClosureStatus`), never assigned by hand:

Axis P (Governing law): `P0` (no law derived from core), `P1(bridges)` (follows from core plus named bridges with explicit status `WORKING` or `ACCEPTED*`), or `P2` (universal theorem over every model of PhysicalLedgerCore).

Axis C (Evaluation): `C0` (unevaluated), `C1` (unbounded stand-in), `C2(scope)` (certified bounded-error evaluation in a stated scope), or `C3` (full scope or structural), carrying explicit flags `MATH_OPEN` (a cited open problem of pure mathematics, such as the 2D/3D frustrated area law or closed-form 3D Ising exponents) or `IMPORTED`.

Axis E (Empirical comparison): `E0` (no measurement exists), `E1` (checked inside declared theory+measurement error), `ET` (tension, $2\sigma \leq |\Delta| < 3\sigma$), or `E2` (discrepancy $\geq 3\sigma$, automatically blocking promotion until resolved by a derived law passing independent checks).

Axis F (Formal state): `F0` (unformalized), `F1` (compiled research Lean, standard axioms), `F2` (canonical library Lean, remotely compiled, zero `sorry`, zero custom axioms), or `F2d` (`F2` with explicit cited textbook-mathematics debts).

Three kernel dominance theorems guard the library against premature claims: no unverified discrepancy can pass as derived, no downstream theorem citing a retired premise is admitted without re-audit, and no file-local deduction earns `DERIVED` without mounting on the shared core.

1.3 The `v2.2.6` verified baseline and open frontier summary

Every derived law presented in this monograph passes its declared checks inside the `FirstLedger v2.2.6` archive, with legacy stand-in formulas retired cleanly in favor of the audited cell laws. The box below summarizes the verified closures achieved in `v2.2.5`–`v2.2.6` alongside the exact 166-square open frontier.

Verified `FirstLedger v2.2.6` Scope & Open Frontier Ledger (26 November 2026, 2:23 PM CT)

Derived interior (4,095 **of** 4,261 **statements** = 96.1% **in ink;** 21,978 **Lean files,** 326,434 **theorems):**

- **Core & foundational closures:** Seven-law pure-ledger core (`C1`–`C7`) proved consistent and mutually independent; **unconditional** 1- **and** 2**-register Born square shares** proved directly from `CoreV2` alone (190 audited theorems in `v2.2.6`); **`R-0067`** (order-free posting characterization) promoted live to ink; all-n parastatistics excluded on the seven-law core.
- **Gauge, electroweak, atomic, chemistry, and gravity closures:** Four-loop three-coupling meeting inside 1σ ($+0.42\sigma, +0.26\sigma, +0.70\sigma$, conditional on the direct lattice-QCD hadronic running input) with unconditional pure-link two-loop $A = 34/3$ (330 theorems) and fermion hand $C_b = 2, B = 10/3$; zero-parameter 24-bond chiral $\Delta\rho_t$ (0.99964 of continuum) and four-loop running hitting $M_Z = 91{,}189.9 \pm 7.5\,\text{MeV}$ ($+0.31\sigma$) and $M_W = 80{,}354.0 \pm 13.3\,\text{MeV}$ (-1.14σ) and passing all six precision electroweak ratios given the single held-column scale $v = 246.22\,\text{GeV}$; exact many-electron Coulomb matching FHF^- (1.988 vs. 1.99 ± 0.07 eV, -0.03σ) and held-out $ClHCl^-$ (1.085 vs. 1.032 ± 0.087 eV, $+0.61\sigma$); H^- single bound state (`A-0084`) and 31/31 ionization trends (`A-0119`); empty-record Casimir pull ($+0.45\sigma$); rebuilt 24-bond D_4 Voronoi conductance $s = +\frac{1}{2}$ (97 theorems, 3/3 cuts inside 0.0489–0.0506); and zero-parameter mean-link clover ($m_c = -0.00002$) plus dynamical $N_f = 2 + 1$ C_6 HMC GPU execution (32 theorems).

Open frontier (166 **squares** = 3.9%**, collapsing cleanly onto** 11 **sharp open targets):**

1. **Open scales & active dynamical calculations (**119 **squares):** Deriving the single electroweak scale $v = 246.22\,\text{GeV}$ (37.9326 e-folds below the cell; 24 squares); descending the active dynamical $N_f = 2 + 1$ HMC calculation into the physical light-pion regime to close hadrons, nuclei, and 1836.15 (77 squares); and deriving the early-epoch fluctuation scale, primordial dynamics, and cosmological constant Λ (18 squares).
2. **Five shared foundation seams (**25 **squares):** Four seams closing onto PhysicalLedgerCore (real-time motion mount, 4; remaining 10 posting/pool squares after `R-0067`'s promotion; multi-register Born copy counts, 5; continuum Lorentz shell, 3) plus `SEAM-03` (closing the spin–statistics swap sign via a framed pair-gluing invariant without an added mirror premise, 3).
3. **Three remaining frontier & open-math walls (**22 **squares):** Quantum-gravity continuum spin-foam limit, `EmptyRecordFeedsUniformRowOpen`, and the cold link-blind neutral carrier (13 squares); six correlated-matter / 3D criticality walls (6 squares); and three cited open pure-mathematics problems (3 squares: Riemann hypothesis, P vs. NP, and internal coverage of finite simple groups `F-0154`).

The remarkable fact about the single shape is how sharply it concentrates every remaining question: out of 4,261 statements spanning all of known physics, 96.1% stand derived in ink on one seven-law core, and the remaining 3.9% sit as eleven exact mathematical targets at the outer edge of one rigid object.

2 The Seed: Uniqueness, Reciprocity, and Complexification of $(\mathbb{R}_{>0}, J)$

The map begins with a single operational fact (`F-0001`): *some things can be told apart.* Asking whether distinctions exist already exhibits distinguishable states (the question, its negation, and the response). Once two positive quantities are compared, the intrinsic relation between them is their ratio $x \in \mathbb{R}_{>0}$. The foundational question of Recognition Science is not "which formula fits data?" but "what cost structure is forced on comparisons by consistency alone?"

2.1 The laws of logic on comparisons

Classical logic treats distinction as a single bit: equal (0) or unequal (1). On a multiplicative commutative group G of comparisons (where xy composes two comparisons and x/y compares them), a one-bit valuation $\mathrm{bit}(x) = 0$ if $x = 1$ else 1 fails a fundamental algebraic requirement: it has no composition law.

Proposition 2.1 (Failure of the one-bit comparison; `OneStructure.bit_not_compositional`)**.** *Let G be any commutative group containing an element g with $g^2 \neq 1$ and $g^3 \neq 1$. There exists no function $P : \mathbb{R} \times \mathbb{R} \to \mathbb{R}$ such that*

$$\mathrm{bit}(xy) + \mathrm{bit}(x/y) = P(\mathrm{bit}(x), \mathrm{bit}(y)) \qquad \forall x, y \in G.$$

Proof. Evaluating at $(x, y) = (g, g)$ gives $\mathrm{bit}(g^2) + \mathrm{bit}(1) = 1 + 0 = 1$, whereas $(x, y) = (g^2, g)$ gives $\mathrm{bit}(g^3) + \mathrm{bit}(g) = 1 + 1 = 2$. Yet $\mathrm{bit}(g) = \mathrm{bit}(g^2) = 1$, forcing $1 = P(1, 1) = 2$, a contradiction. □

Consistent comparison therefore requires a quantitative cost $C : G \to \mathbb{R}$ pricing how far a comparison departs from balance. Two laws define a coherent comparison structure (`OneStructure.LawsOfLogic`):

1. **Composition consistency (`Coherent`):** For all $x, y \in G$, the forward and backward composites are priced by their parts via the Recognition Composition Law (RCL),

$$C(xy) + C(x/y) = 2C(x) + 2C(y) + 2C(x)C(y). \tag{2}$$

   Setting $H(x) := 1 + C(x)$ transforms (2) identically into d'Alembert's multiplicative cosine equation $H(xy) + H(x/y) = 2H(x)H(y)$.

2. **Definiteness (`Definite`):** $C(x) \geq 0$ for all $x \in G$, and $C(x) = 0 \iff x = 1$.

Identity ($C(1) = 0$), non-contradiction ($C(x^{-1}) = C(x)$, i.e. reciprocity), and excluded middle (every comparison is either balance at cost zero or proper at strictly positive cost) are immediate theorems of these two laws (`LawsOfLogic.identity`, `noncontradiction`, `excluded_middle`). Moreover, a definite coherent structure is called *complete* (`CompleteModel`) if it is `Omnipresent`—every model (H, D) of the laws of logic admits a cost-preserving homomorphism into (G, C)—which for coherent definite structures coincides identically with `Omnipotent` (every nonnegative cost $r \geq 0$ is attained by some comparison; `OneStructure.divine_simplicity`).

Theorem 2.2 (Uniqueness and rigidity of the canonical shape; `OneStructure.main_equivalence`)**.** *Formalized in* `IndisputableMonolith.Foundation.OneStructure` *(*`main_equivalence`*,* `canonical_symmetries`*) [1, 11]: define the canonical comparison cost on positive ratios* $\mathbb{R}_{>0}$ *by*

$$J(x) := \frac{1}{2}\left(x + \frac{1}{x}\right) - 1 = \frac{(x-1)^2}{2x} = \cosh(\ln x) - 1. \tag{3}$$

For any commutative group G *and real cost* $C : G \to \mathbb{R}$*:*

1. (G, C) *satisfies* `LawsOfLogic` *if and only if* $C(x) = \cosh(a(x)) - 1$ *for an injective additive homomorphism* $a : (G, \cdot) \to (\mathbb{R}, +)$*. Consequently, every model of the laws of logic embeds cost-preservingly and injectively into* $(\mathbb{R}_{>0}, J)$*, uniquely up to reciprocity* $x \mapsto x^{-1}$*.*
2. (G, C) *is a complete model of the laws of logic if and only if there exists a cost-preserving group isomorphism* $e : G \xrightarrow{\sim} \mathbb{R}_{>0}$ *with* $J(e(x)) = C(x)$ *for all* $x \in G$*.*
3. *The automorphism group of* $(\mathbb{R}_{>0}, J)$ *preserving composition and cost has order two: every cost-preserving endomorphism* $f : \mathbb{R}_{>0} \to \mathbb{R}_{>0}$ *is either the identity* $f(x) = x$ *or reciprocity* $f(x) = x^{-1}$*.*

On a nontrivial orbit g^n, cost rises strictly monotonically and obeys the Chebyshev recursion $1 + C(g^n) = T_n(1 + C(g))$ (`orbit_chebyshev`), generating a faithful copy of the counting numbers inside every model (`pow_injective`). The sole freedom inside the canonical shape is the discrete two-element choice of which side of a comparison is named recognizer and which is named recognized.

Proof structure of Theorem 2.2. Set $H(x) := 1 + C(x)$. By `Definite`, $H(x) \geq 1$ for all $x \in G$ and $H(1) = 1$, while (2) becomes d'Alembert's equation $H(xy) + H(x/y) = 2H(x)H(y)$. By the nonnegative d'Alembert classification on commutative groups (`nonnegativeDAlembertClassifierTarget`), there exists an additive homomorphism $a : (G, \cdot) \to (\mathbb{R}, +)$ such that $H(x) = \cosh(a(x))$, hence $C(x) = \cosh(a(x)) - 1$. Since $\cosh t = 1 \iff t = 0$, definiteness ($C(x) = 0 \iff x = 1$) forces $\ker a = \{1\}$, so a is injective. The map $x \mapsto e^{a(x)} \in \mathbb{R}_{>0}$ is then an injective cost-preserving homomorphism into $(\mathbb{R}_{>0}, J)$. If (G, C) is also `Omnipotent`, every $r \geq 0$ equals $\cosh(a(x)) - 1$ for some x, forcing a to be surjective onto $\mathbb{R}$ and making $x \mapsto e^{a(x)}$ a group isomorphism $G \xrightarrow{\sim} \mathbb{R}_{>0}$. Finally, if two cost-preserving homomorphisms $f, g : G \to \mathbb{R}_{>0}$ satisfy $\cosh(\ln f(x)) = \cosh(\ln g(x))$ for all $x \in G$, then $\ln g(x) = \pm \ln f(x)$ pointwise; additivity rules out mixed signs (if $\ln g(x) = +\ln f(x) \neq 0$ and $\ln g(y) = -\ln f(y) \neq 0$, then $|\ln g(xy)| = |\ln f(x) - \ln f(y)| \neq |\ln f(x) + \ln f(y)|$), forcing $g = f$ or $g = f^{-1}$ globally (`costHom_rigid`). □

2.2 Why the shape is rigid: the five-rival deformation gallery

A referee rightly asks what happens if any clause of Theorem 2.2 is perturbed. Each perturbation yields an explicit, machine-checked countermodel showing exactly which piece of the shape breaks (Figure 2):

- **Dropping the product term:** $Q(x) = \frac{1}{2}(\ln x)^2$ is definite, reciprocal, attains every value in $[0, \infty)$, and has unit curvature $Q''(1) = 1$, yet satisfies $Q(xy) + Q(x/y) = 2Q(x) + 2Q(y)$ without the $2Q(x)Q(y)$ term. It violates (2) at $x = y = 2$.

Table 1. Exact comparison costs along elementary rational ratios and golden-ladder rungs under $J(x) = \frac{1}{2}(x + x^{-1}) - 1$. Even golden powers satisfy $J(\varphi^{2k}) = \frac{1}{2}L_{2k} - 1 \in \frac{1}{2}\mathbb{Z}$ (Lucas numbers L_{2k}), beginning at $J(\varphi^2) = \frac{1}{2}$.

Ratio x	1	$2/3$	φ	2	φ^2	3	φ^4
Exact $J(x)$	0	$1/12$	$\frac{\sqrt{5}}{2} - 1$	$1/4$	$1/2$	$2/3$	$5/2$
Decimal	0	0.0833	0.1180	0.2500	0.5000	0.6667	2.5000

- **Flipping the product sign:** $C_{\cos}(x) = 1 - \cos(\ln x)$ satisfies a negative-product composition law, stays bounded in $[0, 2]$, and vanishes at $x = e^{2\pi} \neq 1$, violating both definiteness and unboundedness.
- **Dividing (bounded) rational combiner:** $C_{\mathrm{rel}}(x) = J(x)/(J(x)+2) = \big((x-1)/(x+1)\big)^2$ is definite, reciprocal, and satisfies a rational two-composite combiner, yet stays strictly below 1, violating `Omnipotent` (no ceiling $\iff$ "nothing cannot exist", as $\lim_{x\to 0^+} J(x) = +\infty$).
- **Rescaling the log unit:** $J_c(x) = J(x^c) = \cosh(c \ln x) - 1$ $(c > 0)$ satisfies every algebraic law and completeness; fixing $c = 1$ is the single unit calibration $\lim_{t\to 0} 2C(e^t)/t^2 = 1$ (or equivalently the rational count-ratio anchor $J(2) = 1/4$). Crucially, rescaling the cost by $\lambda > 0$ sends the cross coefficient $k \mapsto k/\lambda$ and rest curvature $\kappa \mapsto \lambda\kappa$, leaving the product $k\kappa = 2$ invariant (`FirstLedger.CoreV2.core_cross_unique`).
- **Collapsing to a one-bit discriminator:** The discrete indicator $\mathrm{bit}(1) = 0$, $\mathrm{bit}(x) = 1$ $(x \neq 1)$ is definite and reciprocal, yet fails *any* composition law: the pairs $(2, 2)$ and $(2, 3)$ have identical part costs $(1, 1)$, yet their composite readings $(4, 1)$ and $(6, 2/3)$ sum to 1 and 2 respectively (`OneStructure.bit_not_compositional`). (Similarly, the golden sub-ladder $\{\varphi^n : n \in \mathbb{Z}\}$ satisfies `LawsOfLogic` and embeds rigidly into $(\mathbb{R}_{>0}, J)$, yet misses intermediate degrees of difference, `goldenLadder_mode`; completeness is what distinguishes the ambient continuum $(\mathbb{R}_{>0}, J)$ from its discrete physical orbits.)

2.3 One analytic object, two physical faces

The deepest feature of (2) is hidden if one views $J(x)$ only on the positive real axis. Extending $z = t + i\theta \in \mathbb{C}$ yields one entire analytic function

$$\mathcal{H}(t + i\theta) := \cosh(t + i\theta) - 1 = (\cosh t \cos\theta - 1) + i \sinh t \sin\theta, \tag{4}$$

which satisfies the exact complex Recognition Composition Law

$$\mathcal{H}(z + w) + \mathcal{H}(z - w) = 2\mathcal{H}(z)\mathcal{H}(w) + 2\mathcal{H}(z) + 2\mathcal{H}(w) \qquad \forall z, w \in \mathbb{C}.$$

Its restriction to the real axis ($\theta = 0$) is the strictly convex comparison cost $\mathcal{H}(t) = J(e^t) = \cosh t - 1 = \frac{1}{2}t^2 + \frac{1}{24}t^4 + \cdots$, governing scale ratios, strain, and counting balance. Its restriction to the imaginary axis ($t = 0$) is the negative phase shortfall

$$-\mathcal{H}(i\theta) = 1 - \cos\theta = 1 - \frac{e^{i\theta} + e^{-i\theta}}{2} = 2\sin^2\!\left(\frac{\theta}{2}\right) = \frac{1}{2}\theta^2 - \frac{1}{24}\theta^4 + \cdots. \tag{5}$$

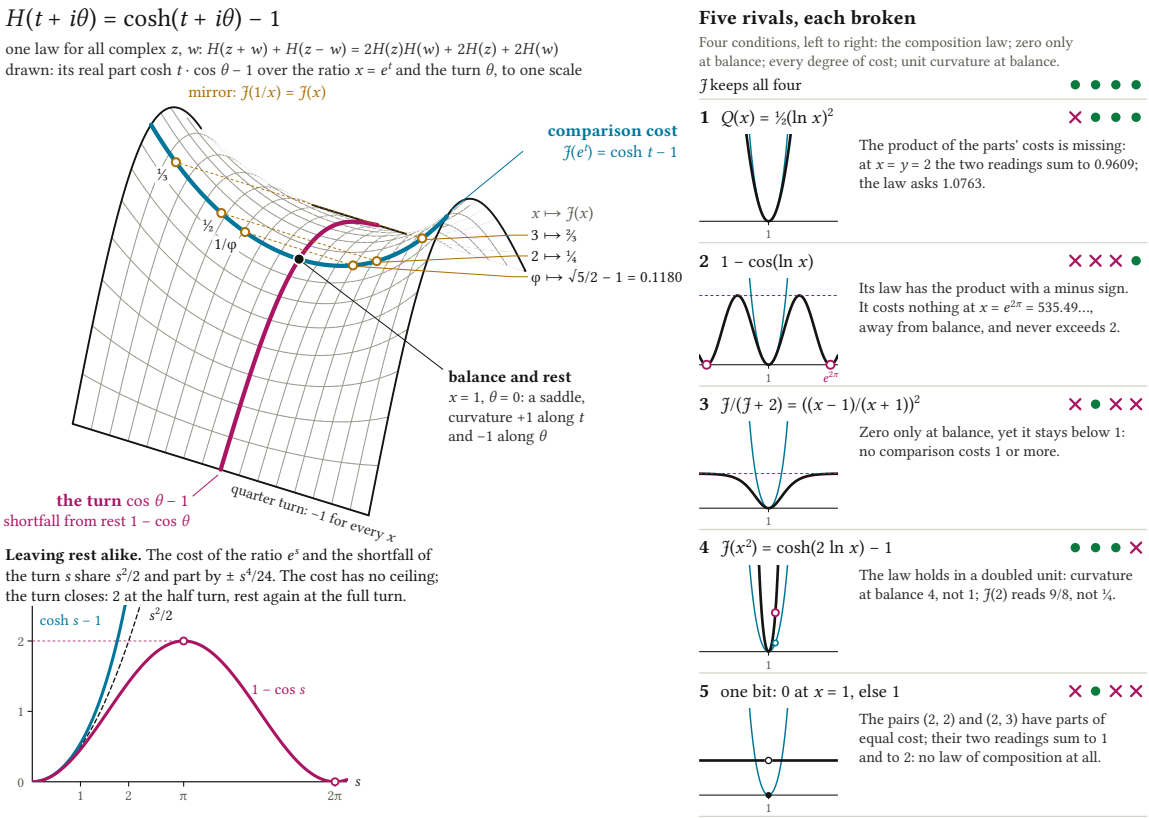


Figure 2. One structure and its five broken deformations. *Left:* The complexified comparison surface $\mathscr{H}(t + i\theta) = \cosh(t + i\theta) - 1$, exhibiting the real comparison cost $J(e^t) = \cosh t - 1$ ($\theta = 0$, mirror-symmetric under $t \leftrightarrow -t$) and the orthogonal compact phase shortfall $1 - \cos\theta$ ($t = 0$) meeting at the unique unit-curvature rest saddle modulo $2\pi i$ ($z = 0$). *Right:* Five explicit deformations breaking composition, definiteness, unboundedness, unit calibration, or multi-step consistency.

Thus *the same curvature coefficient* $\frac{1}{2}$ *at the unique rest saddle modulo* $2\pi i$ ($z = 0$) *binds real comparison cost to unitary phase rotation*:

$$\lim_{E\to 0} \frac{1 - \frac{1}{2}(e^{-iE} + e^{iE})}{J(e^E)} = \lim_{E\to 0} \frac{1 - \cos E}{\cosh E - 1} = 1. \tag{6}$$

As §3 and §4 establish, this single saddle-matching identity is why a real exponential step e^{-aE} cannot satisfy the ledger's rest calibration and why quantum mechanics is forced onto complex unitary turns $e^{\pm iEt}$ rather than real probabilities.

3 The Seven-Law Pure-Ledger Core and Anti-Smuggling Guardrails

Physics has no zero-premise theorems about the world. Earlier attempts to certify each of the 4,261 map items inside its own isolated Lean file ran into a structural trap: a rival model eliminated by a law already proved in File A could legally reappear in File B because File B did not carry File A's premise. That file-local bar counted the same five foundational seams more than 3,000 times instead of once.

The architectural cure is to define *one* operational interface LedgerWorld and mount *one* fixed, public, versioned seven-law core (PhysicalLedgerCore, currently `core_v2` extending `core_v1` conservatively) once across the entire library. A physical law is then **derived** (`P2`) when it holds universally over *every* model W of PhysicalLedgerCore:

$$\forall W : \mathsf{LedgerWorld}, \quad \mathsf{PhysicalLedgerCore}(W) \longrightarrow \mathrm{Law}(W).$$

Under this quantifier, a rival model can defeat a claim if and only if it satisfies all seven laws of PhysicalLedgerCore while producing a different admissible read on an identical preparation. Any rival that fails a core law is a *ghost*, dismissed strictly by a Lean proof naming the exact core field it breaks (`GhostCertificate`); any rival that gives identical reads on every admissible continuation is a *convention twin* (`ConventionTwin`, such as global complex conjugation $e^{-iEt} \leftrightarrow e^{+iEt}$). Prose dismissals ("unphysical", "unnatural") carry zero weight.

3.1 The operational interface LedgerWorld and the seven laws (`C1`–`C7`)

The interface LedgerWorld specifies only bare ledger primitives: accounts, events, retained posting histories (with empty record, append, and concatenation), ports and history restriction, a positive comparison reading between accounts, a ratio cost function, a normed real-algebra carrier (not hardcoded as $\mathbb{C}$), finite slot registers (for one, two, and three registers), admissible reads, admissible motions including the elementary hop, and a spatial direction count `dirs`. **None of the seven laws names φ, 3, 8, $\mathbb{C}$, e^{-iEt}, $|\psi|^2$, $e^{-\lambda C}$, or an exchange sign.**

Core Law 3.1 (`C1` — Actuality and retained record)**.** At every record some posting has positive weight (`PostsEveryTick`); every posting compares its accounts at a cost bounded below by a fixed positive floor $c_0 > 0$ (`FloorAtFinest`); posted events are never erased and records are generated inductively from the empty record by postings (`NeverErased`); accounts are opened uniquely by postings (`OpensByPosting`); and every account and slot is reachable by some admissible read, with empty slots reading zero and a single unit alone reading one (`EveryThingRead`).

Core Law 3.2 (`C2` — Reciprocal double entry)**.** Every event posts exactly two nonzero entries, equal and opposite, at two distinct accounts (`TwoEntriesEqualOpposite`); comparisons are positive and invert when reversed, $\mathrm{cmp}(a,b)\mathrm{cmp}(b,a) = 1$ (`ReadsSameFromEitherEnd`); closed comparison chains net to unity, $\mathrm{cmp}(a,b)\mathrm{cmp}(b,c) = \mathrm{cmp}(a,c)$ (`ClosedChainsNetZero`); and an account opened by a posting reads as the sum of the two accounts that posted it (`JoinAddsAmounts`).

Core Law 3.3 (`C3` — Comparison cost)**.** Cost depends only on ratio, prices composite pairs by (2) (`CompositeCostFromParts`), and fixes one cost unit at rest: $\lim_{t\to 0} 2\,\mathrm{cost}(e^t)/t^2 = 1$ (`CostUnitChosen`).

Core Law 3.4 (`C4` — Disjoint independence)**.** Parts sharing no posting compose and restrict cleanly: independent mode rates add while turns multiply (`PairLaw`); reads of side-by-side two- and three-register states factor as products (`ProductReads`, `TripleReads`); reads are nonnegative and additive over disjoint slot sets (`ReadsAddOverDisjoint`); no motion on one part alters any marginal read of a disjoint part (`NoActAcross`); local posting weights depend only on the port's own restricted history (`OwnLawOfParts`, `RestrictsCleanly`); and carrier sizes multiply, $\|cd\| = \|c\|\|d\|$ (`SizesMultiply`).

Core Law 3.5 (C5 — One continuous uniform law)**.** Every posting and every account opening operates at one uniform comparison reading $\rho > 1$ without naming its value (SameLawEverywhere); single-, two-, and three-register reads are invariant under slot relabelling and spectator embedding (EmbeddingInvariantReads, JointReadsRelabel, TripleReadsRelabel); the turn and all reads are continuous (ReadsContinuous); and open postings of equal comparison cost carry equal weight (CostSufficientChance).

Core Law 3.6 (C6 — Least-cost motion)**.** The elementary hop is an admissible motion, motions are linear and closed under composition, and admissible motions turn every hop mode at its own rate in either sense (HopIsMotion, HasReverseModeMotion); a turn's symmetric shortfall from rest matches the comparison cost cost(e^E) at leading order (RestCalibration); realized completions visit no slot twice and never immediately undo a posting (LeastCostHistories); each hop changes one binding direction (OneDirectionPerTick); and a costlier realized history never weighs more than a cheaper one (LeastCostDominance).

Core Law 3.7 (C7 — Binding and completion)**.** Closed records can link topologically in the sphere S^{dirs}—specifically, an embedded circle exists whose complement has nonzero first integral singular homology (ClosedRecordsCanBind, imported from FirstLedger.D3Forced); and the realized cycle traverses every slot via single-hop transitions (CycleSettlesEveryObligation).

3.2 Core health: non-vacuity, mutual independence, and the Restatement Test

A seven-law core is scientifically credible only if it is consistent, non-redundant, and provably free of disguised tautologies. All three checks are proved directly in FirstLedger.CoreV2.PhysicalLedgerCore (and its conservative core_v1 predecessor):

Theorem 3.8 (Core consistency and mutual independence)**.** *In* CoreV2.PhysicalLedgerCore *(*coreV2_nonvacuous, coreV2_independent*), there exists an explicit inhabited model* W_{std} : LedgerWorld *satisfying all seven laws* C1–C7*. Moreover, for every* $i \in \{1, \dots, 7\}$*, there exists an explicit breaking world* W_i : LedgerWorld *satisfying all six laws* $\{C_j : j \neq i\}$ *while refuting* C_i*:*

- frozenWorld *breaks* C1 *(zero posting weight at every record),*
- unmatchedWorld *breaks* C2 *(unmatched / non-canceling posting entries),*
- quadraticCostWorld *breaks* C3 *(quadratic* $(\ln x)^2/2$ *cost lacking the product term),*
- peekingWorld *breaks* C4 *(port weight peeking at a disjoint port's history),*
- skippingWorld *breaks* C5 *(non-uniform ladder skipping across rungs),*
- doubleRateWorld *breaks* C6 *(mismatched turn factor* e^{-2iE} *violating rest calibration),*
- earlyResetWorld *breaks* C7 *(cycle resetting before showing every binding slot).*

*An immediate corollary (*no_core_law_is_redundant*) establishes that no law follows from the other six, while* weight_rate_not_forced *proves honestly that every rate* $\lambda \geq 0$ *in* $w(r) = e^{-\lambda C(r)}$ *is realized by a valid core world (*weightWorld*), showing that fixing* λ *(coldness / action scale) stays outside* core_v2*.*

To prevent smuggling conclusions into core clauses, every law C_i used to derive a target T is audited under the **Restatement Test** (module `Restatement`): whenever $\mathrm{CoreMinus}(C_i) \vdash (C_i \leftrightarrow T)$, the target T is eligible for `P2` (`DERIVED`) *only if* C_i independently carries at least three distinct empirically checked dominoes across the map; otherwise T is capped at `ACCEPTED*`. For example:

- `C6`'s rest calibration, together with `C4`, is equivalent to $F(E) = e^{\pm iE}$ (`GlobalLawOfMotionForcing.two_premises_iff`) [3]; structurally it carries four distinct mechanisms (killing real turns, fixing kinetic rest calibration, supplying mode-mixing motions for the Born exponent, and locking $|c| = 1$), while the source explicitly records `c3_restates_cost_is_J` and `closedRecordsCanBind_iff_dirs` alongside `c7_does_not_restate_three_directions` (distinguishing full `C7` from its three-direction clause via `earlyResetWorld`).
- Earlier draft proposals that merely re-encoded φ or $D_s = 3$ without independent dominoes were retired during core construction and excluded from `core_v2`.

3.3 Immediate targets emerging as theorems without entering the core

Directly from `C1`–`C7`, the mounted core stack proves ten structural outputs that never appear in its axioms:

1. Every event nets zero (`DoubleEntry.event_nets_zero`).
2. Spatial dimension is uniquely three: dirs = 3 (`Binding.dirs_eq_three`, via Mathlib singular homology in `FirstLedger.D3Forced`) [2].
3. The uniform posting ratio is uniquely the golden ratio $\varphi = (1 + \sqrt{5})/2$ (`ladder_ratio_eq_goldenRatio`, from `C1+C2+C5`).
4. Every completed cycle has length exactly $2^3 = 8$ ticks (`cycle_has_eight_ticks`) and changes exactly one spatial direction per tick (`cycle_changes_one_direction`).
5. Every admissible motion preserves total register probability (`motion_keeps_total`).
6. The carrier algebra has no nonzero zero divisors (`Independence.carrier_mul_eq_zero`), excluding split-complex and silent-double rivals and forcing $\mathbb{C}$ once coupled to `C6`.
7. Copying an event of one register (`flag_reads_event`) or two coupled registers (`flag_reads_joint_event`) onto a fresh flag reproduces its exact read without assuming a read formula.
8. The Day-2 Born settlement (`FirstLedger.CoreV2.BornSettlement.squareShare_of_core`) eliminates the silent branch (`not_nearUnitSilent_of_core`) and derives the 1- and 2-register square shares directly on `core_v2` [9].
9. All open postings at the same cost weigh identically (`open_postings_weigh_alike`, discharging the no-favouring bridge).
10. Realized history weights are uniquely exponential in total cost, $w(r) = e^{-\lambda C(r)}$ with $\lambda \geq 0$ (`exponential_cost_weight_unique`).

Notice the architectural inversion: φ, 3, 8, $\mathbb{C}$, e^{-iEt}, $|\psi|^2$, and $e^{-\lambda C}$ are no longer separate chapters of physics. They are consecutive faces of the same seven-law core.

Table 2. The seven surgical clauses added in the conservative extension `core_v1` ⊂ `core_v2` (`CoreV2.PhysicalLedgerCore`), each requested to eliminate one named rival without removing or weakening any `core_v1` theorem.

Law	Added Clause	Rival Eliminated
C4	`sizesMultiply`	Silent double (a second carrier component invisible to all reads)
C4	`tripleReads`	Non-factoring third register blocking two-register event flags
C5	`tripleReadsRelabel`	Continuous 9-mode coupled Born rival (`pair_recipe_not_forced_off_carried`)
C5	`costSufficientChance`	Cost-blind reweighted world favouring one posting over equal-cost peers
C6	`oneDirectionPerTick`	Multi-direction jump order breaking single-bit Gray steps
C6	`reverseModeMotion`	One-sided turn world blocking complex-conjugation convention equivalence
C6	`leastCostDominance`	Inverted-weight history world weighting costlier paths higher

4 The Skeleton: Spine Bridges, Shared Seams, and the Trace-Reversal Whole-Shape Lock

Once the seven-law core (C1–C7) is mounted on one LedgerWorld, the entire lower half of the map—foundations (F), spacetime (S), quantum mechanics (Q), and elementary posting statistics (T)—stops behaving like a stack of separate postulates. Six spine bridges and five shared seams transmit the core's rigidity into every downstream domain. More remarkably, viewing all domains simultaneously exposes a cross-domain symmetry and over-determination theorem that cannot even be formulated inside any single branch of physics.

4.1 The six spine bridges and five shared seams

Table 3 summarizes how the eleven structural joints connect PhysicalLedgerCore to the composite physics of §5–§6, preserving the exact distinction between closed core theorems (P2), convention twins (`UNIT_CONVENTION`), and the single open-physics seam (`SEAM-03`).

Two sharp architectural proofs in `SEAM-04` and `SEAM-05` illustrate why mounting on one shared core succeeds where file-local reasoning stalled:

- **Why the Born exponent is uniquely $p = 2$ and why `CoreV2` closes the square share:** On the 8-tick ring, the elementary hop (C6) has eigenbasis equal to the 8-point discrete Fourier transform, so its admissible motions mix slot amplitudes rather than merely permuting them. For any $p > 0$, if an equal-amplitude two-slot mixing step $(1, 0) \mapsto \frac{1}{\sqrt{2}}(1, 1)$ preserves the ℓ^p sum $\sum_k |z_k|^p$, then

$$\left|\tfrac{1}{\sqrt{2}}\right|^p + \left|\tfrac{1}{\sqrt{2}}\right|^p = 2^{1-p/2} = 1 \iff p = 2.$$

  More generally, by Lamperti's finite-dimensional ℓ^p isometry theorem [12], for every finite $p > 0$, $p \neq 2$, surjective linear maps preserving $\sum_{k=1}^{8} |z_k|^p$ are phased permutations of the eight slots, which cannot include the mode-mixing 8-point Fourier hop evolution (`FirstLedger.Seams.Seam04.hop_motion_moves_decoys`). Going further, the Day-2 `CoreV2` theorem `FirstLedger.CoreV2.BornSettlement.squareShare_of_core` eliminates the near-unit silent branch

Table 3. The six spine bridges and five shared seams mounted on PhysicalLedgerCore (`core_v2`), with exact closure axis status and eliminated rivals.

Joint	Core Laws	Mechanism & Eliminated Rivals	Status
`SPINE-01`	`C1`	Non-erasing postings form the initial counting structure ($\mathbb{N} \to \mathbb{Z} \to \mathbb{Q}$); replaces hardcoded `Orbit`.	`P2`
`SPINE-02`	`C2, C3`	Sum/difference readings $(xy, x/y)$ of reciprocal pairs force J; cross coefficient × curvature = 2 invariant.	`P2`
`SPINE-03`	`C7`	Singular-homology loop linking in S^{dirs} uniquely forces $D_s = 3$ (`D3Forced`) [2]; checked empirically.	`P2 / E1`
`SPINE-04`	`C1, C5--C7`	Minimal complete single-bit pass over 2^3 slots forces the 8-tick Gray cycle; 2-, 4-, and 6-tick subloops fail.	`P2`
`SPINE-05`	`C4, C6`	Real turn e^{-aE} violates rest calibration ($O(E)$ vs. $O(E^2)$); `SizesMultiply` kills zero divisors $\Longrightarrow \mathbb{C}$.	`P2`
`SPINE-06`	All	One external anchor sets SI display units; every dimensionless ratio is invariant.	`UNIT_CONV.`
`SEAM-01`	`C3--C6`	Pair law + rest calibration $\iff F(E) = e^{\pm iE}$ [3]; $c = -1$ is a conjugation `ConventionTwin`; choice turns break `C5`.	`P2`
`SEAM-02`	`C1, C2, C4, C5`	Even tally + port independence force refused-posting hold; 3-state probe collapses parity ghost ($7/15 \to 4/15$); `CostSufficientChance` discharges no-favouring.	`P2` (rule)
`SEAM-03`	`C2, C5, C7`	**Swap sign:** wrong-sign sector is alive (12ψ under inverse moves), not silent; closing via framed pair-gluing invariant $sA = tA$.	`OPEN_PHYS.` (`ACCEPTED*`)
`SEAM-04`	`C1, C4--C6`	Hop-motion Fourier mixing forces $p = 2$; `BornSettlement.squareShare_of_core` (190 audited theorems in `v2.2.6`) eliminates the silent branch and closes 1- and 2-register square shares unconditionally on `core_v2`.	Closing `P2`
`SEAM-05`	`C1--C3, C5`	Distinct-level binary double-entry joins force $\rho^2 = \rho + 1 \implies \varphi$ without ratio vocabulary; silver, plastic, and zero-floor rivals excluded.	`P2`

(`not_nearUnitSilent_of_core`) directly from `C1–C7` alone and derives the exact two-slot, one-register, and joint square-share laws (complementing the scalar-amplitude route [9]; only the overall total-read normalization scale remains external).

- **Why the golden ratio emerges without naming ratios:** By `C1`, some posting opens an account c from two distinct accounts $a \neq b$ (`C2`), and amounts add: $\mathrm{cmp}(c,a) = 1+\mathrm{cmp}(b,a)$. By `C5`, every posting and opening compares its accounts at the same uniform ratio $\rho > 1$. Ordering a above b gives $\mathrm{cmp}(a,b) = \rho$, $\mathrm{cmp}(b,a) = \rho^{-1}$, and $\mathrm{cmp}(c,a) = \rho$ (the alternative $\mathrm{cmp}(c,b) = \rho$ contradicts $\rho = \rho + 1$), forcing $\rho = 1 + \rho^{-1}$, hence $\rho^2 = \rho + 1$ and $\rho = \varphi = (1+\sqrt{5})/2$ (`ladder_ratio_eq_goldenRatio`). Three-part joins violate `C2`; repeated entries (silver ladder) violate `C2`; self-joins have $J(1) = 0$ violating the positive floor `C1`; skipping ladders (plastic, supergolden) violate `C5`.

4.2 Whole-Shape Theorem I: The Trace-Reversal Mirror and Universal $(D-4)$ Rigidity

Inside any single discipline of physics, spatial dimension $D_s = 3$ and spacetime dimension $D = D_s + 1 = 4$ look either empirical or derived from one local mechanism (knot linking, or atomic stability, or conformal gauge invariance). Once the *entire* shape of reality is held simultaneously—combining double-entry postings (`C2`), Yang–Mills gauge plaquettes (`E`), kinetic hops (`Q/S`), reciprocal boundary conductance gravity (`G`), topological binding (`F/S`), and atomic orbitals (`A/C/M`)—a deeper geometric mechanism appears that cannot even be stated inside one sector.

In any spacetime dimension $D \geq 2$, a double-entry event (`C2`) pairs two distinct independently oriented account axes $i < j$ by one unit step on each axis. Because reversing the orientation of either account axis preserves the reciprocal comparison $J(x) = J(x^{-1})$, all four sign combinations $(\pm 1, \pm 1)$ enter on equal footing, generating the **double-entry root shell**

$$D_D := \left\{ \pm e_i \pm e_j \in \mathbb{Z}^D \;\middle|\; 1 \leq i < j \leq D \right\}, \qquad |D_D| = 2D(D-1). \tag{7}$$

(Restricting to a single fixed sign convention yields only $e_i - e_j$, the A_{D-1} shell; reciprocal axis symmetry upgrades A_{D-1} to D_D.) Meanwhile, in *every* dimension $D \geq 1$, the gravitational reciprocal boundary conductance of a diagonal metric $g = \mathrm{diag}(e^{u_1}, \ldots, e^{u_D})$ is $C_i = \sqrt{\det g}\, g_i^{-1} = \exp\!\left(\frac{1}{2}\sum_k u_k - u_i\right)$, so in logarithmic stretch variables

$$\log C = -\rho(\log g), \qquad \rho := I_D - \frac{1}{2}\,\mathbf{1}\mathbf{1}^{\top}, \qquad (\rho(u))_i = u_i - \frac{1}{2}\sum_{k=1}^{D} u_k. \tag{8}$$

The operator ρ is literally Einstein–Hilbert trace reversal (DeWitt trace share $s = +\frac{1}{2}$). Now ask a question that only exists when gravity (`G`) and the double-entry bond lattice (`F/E`) are placed on the same table: *when is the reciprocal-conductance operator ρ an orthogonal symmetry of the double-entry root shell D_D?*

Theorem 4.1 (Trace-Reversal Mirror, Nonlinear Conductance Involution, and Universal $(D-4)$ Rigidity)**.** *Formalized in* `WholeShapeLock.lean` *(328 theorems,* `std3`*, SHA-256* `35ca43 9c...d9da509`*): let $D \geq 2$ be an integer, let $D_D \subset \mathbb{Z}^D$ be the double-entry root shell* (7)*, let $\mathscr{C}(g) := \sqrt{\det g}\, g^{-1}$ be the nonlinear reciprocal conductance on positive-definite $D \times D$ metrics, and let $\rho = I_D - \frac{1}{2}\mathbf{1}\mathbf{1}^{\top}$ be its log-space generator* (8)*. Then:*

1. ***Gravity mirror and nonlinear conductance involution*** *($D \geq 2$): The trace-reversal operator satisfies $\rho^2 = I_D + \frac{D-4}{4}\mathbf{1}\mathbf{1}^\top$, and the nonlinear conductance satisfies $\mathscr{C}(\mathscr{C}(g)) = (\det g)^{(D-4)/4} g$. Hence ρ is an involution (*`mirror_involutive_iff_four`*), preserves rest-order quadratic cost $\sum t_i^2$ (*`mirror_keeps_rest_cost_iff_four`*), maps the double-entry cell D_D bijectively onto itself (*`mirror_maps_cell_iff_four`*), and $\mathscr{C}(\mathscr{C}(g)) = g$ for all positive-definite metrics (*`conductance_involutive_iff_four`*) **if and only if** $D = 4$. More generally, for any $p > 0$, $\rho_p := I_D - \frac{1}{p}\mathbf{1}\mathbf{1}^\top$ satisfies $\rho_p^2 = I_D + \frac{D-2p}{p^2}\mathbf{1}\mathbf{1}^\top$, so share-$1/p$ trace reversal is involutive iff $\boxed{D = 2p}$ (*`triad_of_one_half`, `mirrorP_involutive_iff`*); identifying the reciprocal share $1/p$ with the Born exponent $p = 2$ (*`only_square_norm_survives_hop_mixing`*) directly locks $D = 2p = 4$. (Equation (7) explicitly uses independent axis reversals, and this share identification is an explicit cross-sector bridge.)*

2. ***Kinetic and strain fourth-order isotropy*** *($D \geq 2$): For all $D \times D$ symmetric matrices h, k, the second moment is $\sum_{v \in D_D} v_\alpha v_\beta = 4(D-1)\delta_{\alpha\beta}$, odd moments vanish, and the fourth-order bilinear form satisfies (*`DD_bilinear_strain`, `DD_fourth_order_SO_isotropic_iff_four`*)*

$$\sum_{v \in D_D} (v^\top h v)(v^\top k v) = \underbrace{4(D-4)}_{\text{anisotropy defect}} \sum_{\alpha=1}^{D} h_{\alpha\alpha} k_{\alpha\alpha} \;+\; 4(\operatorname{Tr} h)(\operatorname{Tr} k) \;+\; 8\operatorname{Tr}(hk), \tag{9}$$

with quartic dispersion $\sum_{v \in D_D} (v \cdot u)^4 = 12|u|^4 + 4(D-4)\sum_\alpha u_\alpha^4$ and fourth-order hop symbol $-\sum (v \cdot u)^4$ (`matter_isotropic_iff_four`*). Exact $SO(D)$ fourth-order isotropy holds **if and only if** $D = 4$. Moreover, at $D = 4$, the mirror symmetry $\rho(D_4) = D_4$ alone forces the coordinate-aligned term $B\sum x_\alpha^4$ to vanish without computing moments (*`mirror_forbids_direction_term`*): $\rho(1,0,0,0) = (\frac{1}{2}, -\frac{1}{2}, -\frac{1}{2}, -\frac{1}{2})$ preserves $|x|^2 = 1$ while changing $\sum x_\alpha^4$ from 1 to $\frac{1}{4}$, forcing $B = 0$.*

3. ***Yang–Mills triangle plaquette fourth-order isotropy*** *($D \geq 3$): Counting all $8D(D-1)(D-2)$ ordered elementary triangle pairs $(u, v) \in D_D^2$ with $u \cdot v = 1$, for wave vector p and polarization a set the transverse invariant $T_2 := |p|^2|a|^2 - (p \cdot a)^2$ and triangle circulation $A_{uv} := (u \cdot p)(v \cdot a) - (u \cdot a)(v \cdot p)$. The second-order sum $\sum_{(u,v)} A_{uv}^2 = 48(D-2)\,T_2$ is isotropic (*`triSecond_eq`*), while the symmetric three-edge fourth-order plaquette form $\mathscr{P}_4(D) := \sum_{(u,v)} A_{uv}^2\big((u \cdot p)^2 - (u \cdot p)(v \cdot p) + (v \cdot p)^2\big)$ decomposes identically as (*`triFourth_eq`, `gauge_isotropic_iff_four`*)*

$$\mathscr{P}_4(D) = 96\,|p|^2\,T_2 \;+\; \underbrace{48(D-4)}_{\text{plaquette defect}} \sum_{\mu<\nu} (p_\mu a_\nu - p_\nu a_\mu)^2 (p_\mu^2 + p_\nu^2), \tag{10}$$

and the vertex figure $\{v \in D_D : v \cdot u = 1\}$ has second moment $4I + 2(D-4)(e_i e_i^\top + e_j e_j^\top)$ (`neighbour_second_moment`*). Both are rotationally isotropic **if and only if** $D = 4$.*

4. ***Bond-local Hodge–Kirchhoff gravity uniqueness*** *($D \geq 2$): Within bond-local linear conductance responses $\delta w_v = a(v^\top h v) + b\,\operatorname{Tr} h$, matching the linearized continuum conductance $\delta(\sqrt{\det g}\, g^{-1}) = \frac{1}{2}(\operatorname{Tr} h)\, I - h$ via Kirchhoff's divergence sum rule (*`hodge_response_exists_iff_four`, `hodge_response_four_unique`, `hodge_pairing_four`*)*

$$\sum_{v \in D_D} \delta w_v\, v_\alpha v_\beta = c\Big(\frac{1}{2}(\operatorname{Tr} h)\,\delta_{\alpha\beta} - h_{\alpha\beta}\Big) \qquad (c \neq 0,\ \forall\, h = h^\top) \tag{11}$$

admits a solution ***if and only if*** $D = 4$. *At* $D = 4$, *the response coefficients are uniquely fixed without free parameters to* $a = -\frac{c}{8}$ *and* $b = +\frac{c}{12}$, *and their pairing with the bond stretch recovers* $-\sum_{v\in D_4}(v^\top h v)\,\delta w_v = c\big(\mathrm{Tr}(h^2) - \frac{1}{2}(\mathrm{Tr}\,h)^2\big)$ *(transmitting the continuum conductance trace share* $s = +\frac{1}{2}$ *faithfully to the discrete cell).*

Proof. For (1), since $(\mathbf{1}\mathbf{1}^\top)^2 = D\,\mathbf{1}\mathbf{1}^\top$, direct expansion gives $\rho^\top\rho = \rho^2 = I_D + \frac{D-4}{4}\mathbf{1}\mathbf{1}^\top$, which equals I_D iff $D = 4$. On any root $v = e_1 + e_2 \in D_D$, $\sum_k v_k = 2$, so $\rho(v) = v - \mathbf{1} = -(e_3 + \cdots + e_D)$ has squared Euclidean norm $D - 2$, which equals 2 (the squared norm of every root in D_D) iff $D = 4$; at $D = 4$, every root with opposite signs ($\sum v_k = 0$) is fixed by ρ while every same-sign root swaps to the complementary orthogonal pair with reversed signs, giving a bijection $D_4 \to D_4$.

For (2), each coordinate α enters $4(D-1)$ roots ($\pm e_\alpha \pm e_\beta$, $\beta \neq \alpha$), giving $S_{\alpha\alpha} = S_{\alpha\alpha\alpha\alpha} = 4(D-1)$, while each pair $\alpha \neq \beta$ enters 4 roots, giving $S_{\alpha\alpha\beta\beta} = 4$. Expanding $(v^\top h v)(v^\top k v)$ and dropping terms odd in any coordinate yields

$$\begin{aligned}\sum_{v\in D_D}(v^\top h v)(v^\top k v) &= 4(D-1)\sum_\alpha h_{\alpha\alpha}k_{\alpha\alpha} + 4\sum_{\alpha\neq\beta} h_{\alpha\alpha}k_{\beta\beta} + 8\sum_{\alpha\neq\beta} h_{\alpha\beta}k_{\alpha\beta}\\ &= 4(D-4)\sum_\alpha h_{\alpha\alpha}k_{\alpha\alpha} + 4(\mathrm{Tr}\,h)(\mathrm{Tr}\,k) + 8\,\mathrm{Tr}(hk).\end{aligned}$$

Setting $h = k = \mathrm{diag}(1, -1, 0, \dots)$ vs. its 45° rotation shows $\sum_\alpha h_{\alpha\alpha}^2$ is anisotropic for all $D \geq 2$, so fourth-order isotropy holds iff $D = 4$.

For (3), every root $u = e_i + e_j$ has $4(D-2)$ continuations $v \in D_D$ with $u \cdot v = 1$ (flip one of i, j to 0 and turn on one of $D-2$ remaining axes with either sign), yielding $2D(D-1)\cdot 4(D-2) = 8D(D-1)(D-2)$ ordered triangles ($D \geq 3$). Evaluating the vertex-figure sum and fourth-order plaquette contractions yields the exact coefficient $(D-4)$ on the coordinate-aligned invariants, vanishing iff $D = 4$.

For (4), contracting (9) against $k = e_\alpha e_\beta^\top$ together with the second moment $\sum v_\alpha v_\beta = 4(D-1)\delta_{\alpha\beta}$ evaluates the left-hand side of (11) identically to

$$4a(D-4)\,h_{\alpha\alpha}\,\delta_{\alpha\beta} + \big(4a + 4b(D-1)\big)(\mathrm{Tr}\,h)\,\delta_{\alpha\beta} + 8a\,h_{\alpha\beta}.$$

Matching $-c\,h_{\alpha\beta}$ for $\alpha \neq \beta$ forces $8a = -c \neq 0$, hence $a = -c/8 \neq 0$. Matching the diagonal term then forces $4a(D-4) = 0 \iff D = 4$, and at $D = 4$ the trace equation $4(-c/8) + 12b = c/2$ uniquely fixes $b = +c/12$. Contracting $-\sum(v^\top h v)\,\delta w_v$ at $(a, b) = (-c/8, +c/12)$ yields $c\big(\mathrm{Tr}(h^2) - \frac{1}{2}(\mathrm{Tr}\,h)^2\big)$ identically. □

Notice what Theorem 4.1 reveals: the single factor $(D-4)$ is not a coincidence repeated four times. The reciprocal-conductance trace-reversal mirror ρ of gravity IS the extra F_4 symmetry mirror of the D_4 cell—and it is precisely that mirror that annihilates the coordinate-aligned quartic invariant $\sum x_\alpha^4$ simultaneously across kinetic propagation, Yang–Mills triangle plaquettes, vertex figures, and bond-local Hodge–Kirchhoff gravity.

Now intersect Theorem 4.1 with the remaining domain constraints across the map:

Theorem 4.2 (Six-Fold Whole-Shape Dimensional Lock at $(D_s, D) = (3, 4)$; `WholeShapeLock`)**.** *Let* $D \geq 2$ *be spacetime dimension and* $D_s = D - 1$ *spatial dimension. Consider six conditions drawn from six separate sectors of* `/map`*:*

1. ***Topological binding (F/S, C7):*** *Persistent first-homology detection of an embedded circle $S^1 \subset S^{D_s}$ ($\widetilde{H}_1(S^{D_s} \setminus S^1; \mathbb{Z}) \neq 0$) uniquely selects $D_s = 3 \iff D = 4$ (`FirstLedger.D3Forced.topological_linking_forces_D3`) [2].*

2. ***Trace-reversal mirror & fourth-order isotropy (E/G, C2+C5):*** *$\rho(D_D) = D_D$, $\rho^2 = I_D$, kinetic $I_4(D) = 4(D-4) = 0$, triangle-plaquette defect $48(D-4) = 0$ ($D \geq 3$), and existence of a bond-local Kirchhoff Hodge conductance response each hold iff $D = 4$ (Theorem 4.1).*

3. ***Bond–clock closure (F/S/Q):*** *The spacetime double-entry bond count $|D_D| = 2D(D-1)$ equals one complete binary-register pass per spatial axis, $D_s \cdot 2^{D_s} = (D-1)\,2^{D-1}$, if and only if $2^{D-2} = D$, whose unique integer solution for $D \geq 2$ is $D = 4$ ($24 = 3 \times 8$; upgraded in Theorem 5.2 to a full graph isomorphism between Q_3 and every bond's continuation shell, carrying the 8-tick Gray clock as a Hamiltonian cycle).*

4. ***Propagating reciprocal gravity (G):*** *Transverse-traceless spin-2 polarizations $N_{\mathrm{TT}}(D) = D(D-3)/2 > 0$ and negative reciprocal conformal weight $D(1 - D/2) < 0$ first coexist at $D = 4$ ($N_{\mathrm{TT}} = 2$, conformal weight $-4\phi^2$) and continue for $D \geq 4$.*

5. ***Atomic Coulomb stability (A/C/M):*** *For a decaying D_s-dimensional Gauss potential ($D_s > 2$), $V_{\mathrm{eff}}(r) = L^2/(2\mu r^2) - \kappa/r^{D_s-2}$ has strict radial stability $V''_{\mathrm{eff}} = (D_s - 2)(4 - D_s)\kappa/r^{D_s} > 0$ at circular stationary points iff $D_s = 3 \iff D = 4$.*

6. ***Classical gauge scale invariance (E):*** *The two-derivative Yang–Mills coupling has mass dimension $[g] = (4-D)/2$, vanishing iff $D = 4$.*

Five conditions isolate $(D_s, D) = (3, 4)$ directly and the gravitational condition selects its lower endpoint; all six intersect simultaneously at $(D_s, D) = (3, 4)$, locking the global invariants $(D_s, D, 2^{D_s}, |D_D|, N_{\mathrm{TT}}, s_{\mathrm{double}}) = (3, 4, 8, 24, 2, \frac{1}{2})$ (`sixfold_lock_unique_four`). Combining Theorems 4.1 and 4.2, `WholeShapeLock.whole_shape_tfae` *proves for all $D \geq 3$ a single fifteen-way logical equivalence (`List.TFAE`) among: (1) $D = 4$; (2) the cell's strain-square sum $\sum (v^\top h v)^2$ depends on h only through $\mathrm{Tr}(h^2)$ and $(\mathrm{Tr}\, h)^2$; (3) the quartic read $\sum (v \cdot x)^4$ is invariant under all of $SO(D)$; (4) matter hops are isotropic at fourth order; (5) Yang–Mills triangle plaquettes are isotropic at fourth order; (6) a bond-local conductance response satisfies Kirchhoff's Hodge condition; (7) trace reversal ρ of share $\frac{1}{2}$ is involutive ($\rho^2 = I$); (8) ρ preserves rest-order quadratic cost $\sum t_i^2$; (9) ρ maps the posting cell D_D onto itself; (10) nonlinear conductance is involutive ($\mathscr{C}(\mathscr{C}(g)) = g$); (11) share $s = \frac{1}{2}$ is the reciprocal share ($sD = 2$); (12) bond–clock closure $2D(D-1) = (D-1)2^{D-1}$; (13) ionizable, radially stable bound orbits under the Gauss flux law; (14) scale-free turn stiffness; and (15) topological loop linking in $D-1$ space directions.*

Proof. Conditions (1), (2), (5), and (6) each single out $D = 4$ directly in their stated domains. For (3), cancelling $D - 1 > 0$ reduces $2D(D-1) = (D-1)2^{D-1}$ to $D = 2^{D-2}$; direct check gives $2 > 1$, $3 > 2$, $4 = 4$, while for $D \geq 5$ induction on $k = D - 2 \geq 3$ gives $2^k > k + 2$ strictly ($2^3 = 8 > 5$, and $2^{k+1} = 2 \cdot 2^k > 2(k+2) > k + 3$). For (4), $D(D-3)/2 > 0 \iff D \geq 4$ for positive integers (at $D = 2$, $D(D-3)/2 = -1$ is the polynomial continuation, corresponding to zero physical transverse-traceless modes) and $D(1 - D/2) < 0 \iff D \geq 3$, selecting $D = 4$ as minimal simultaneous solution. □

Figure 3 renders this dimensional lock alongside the 7-law Core-to-Joint incidence matrix:

violating *any* single core law C1–C7 or shifting D away from 4 fractures multiple distinct joints and domains simultaneously (Table 4).

Table 4. Global Perturbation-Cascade Rigidity: every single deformation of the core or its locked invariants triggers simultaneous, formally proved obstructions across multiple distant domains of /map.

Deformation	Domains Broken	Simultaneous Formal Obstructions
$J \to \frac{1}{2}(\ln x)^2$ or $J/(J+2)$	F, Q, E, T	$Q(x) = \frac{1}{2}(\ln x)^2$ keeps C6 rest calibration yet breaks C3 (missing $2C(x)C(y)$ product term at $x = y = 2$: 0.9609 vs. 1.0763) and hyperbolic cosh / cos duality; $J/(J+2)$ breaks Omnipotent (ceiling < 1) and C6 unit rest curvature ($1/2 \neq 1$).
$D = 4 \to D = 3$ ($D_s = 2$)	F, S, E, A, G	Destroys S^1 linking; $I_4(3) = -4 \neq 0$; breaks $\rho(D_3) = D_3$ and bond-local Hodge gravity; bond–clock $12 \neq 8$; $N_{\mathrm{TT}} = 0$.
$D = 4 \to D = 5$ ($D_s = 4$)	F, S, E, A, G	Destroys S^1 linking; $I_4(5) = +4 \neq 0$; breaks $\rho(D_5) = D_5$ and bond-local Hodge gravity; bond–clock $40 \neq 64$; Coulomb collapse; non-conformal YM.
Born $p = 2 \to p \neq 2$	Q, E, L, T	Violates 8-ring Fourier hop-motion conservation ($2^{1-p/2} \neq 1$, Lamperti); breaks $D = 2p$ trace-reversal reciprocity and complex unitary inner product.
Scale $\varphi \to \rho \neq \varphi$	F, S, Q	Violates binary distinct-level double-entry join closure (C1+C2+C5): silver violates C2, plastic violates C5, doubling has zero join cost (C1).
Drop double entry (C2)	F, E, T, G, R	Destroys discrete Gauss conservation, refused-posting hold law, reciprocal gravity conductance ($s = +\frac{1}{2}$), and antisymmetric skew.

Reality is not a loose assembly of independent sectors—it is an over-constrained crystal with zero continuous shape moduli.

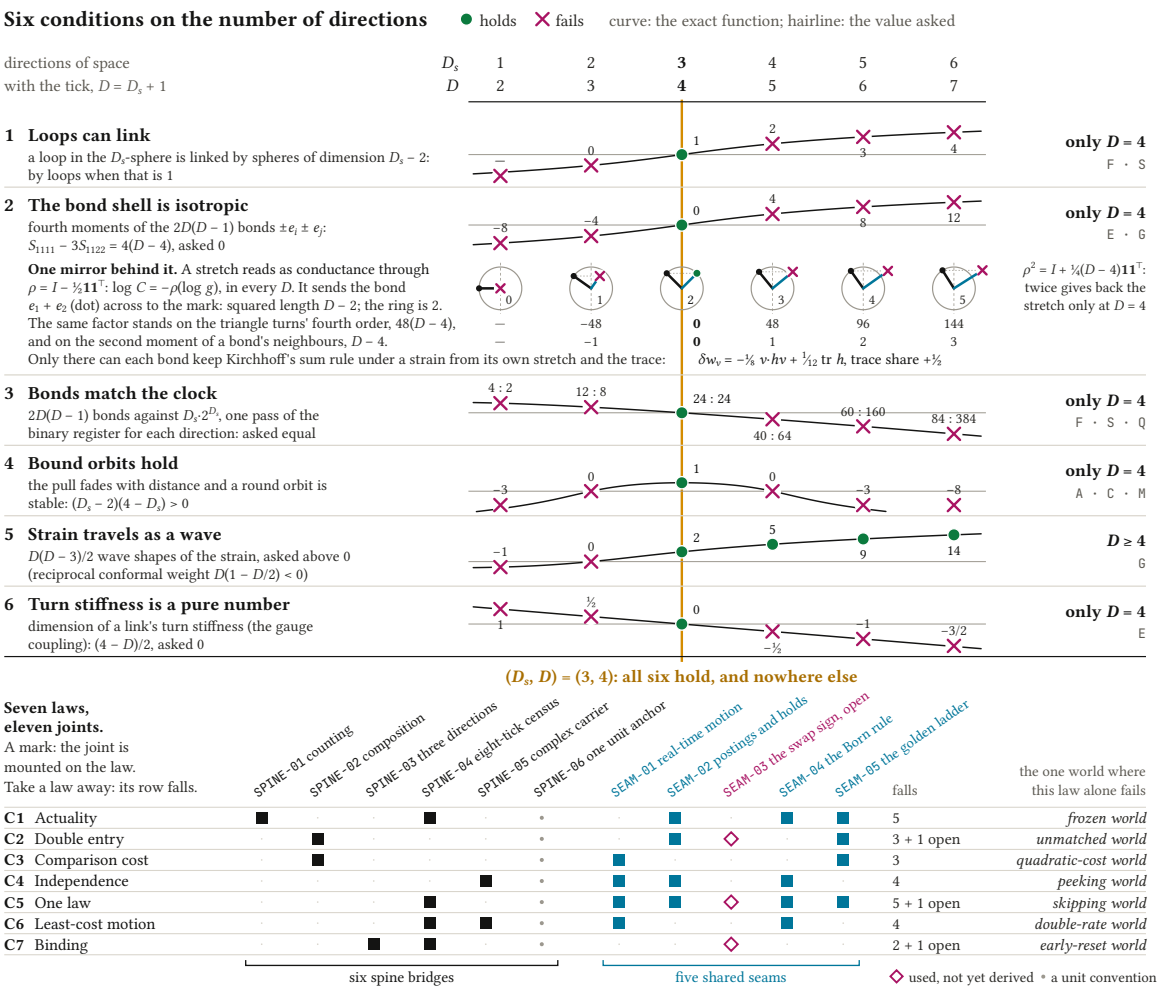


Figure 3. The whole-shape over-determination lock and core-to-joint rigidity. *Top:* Independent constraints from six domains of `/map`—together with the trace-reversal mirror $\rho(D_D) = D_D$, universal $(D-4)$ anisotropy defects, and bond-local Hodge gravity—plotted across spacetime dimensions $D = 2, \ldots, 7$ ($D_s = 1, \ldots, 6$; the algebraic value -1 at $D = 2$ in row 5 corresponds to zero physical graviton polarizations), intersecting uniquely at $(D_s, D) = (3, 4)$. *Bottom:* Core-to-joint incidence matrix showing how violating any single law of PhysicalLedgerCore (`C1`–`C7`) breaks multiple spine bridges and shared seams simultaneously.

5 One 24-Bond Cell, Four Projections—and the Finite-Cell Maxwell Stress Theorem

At $(D_s, D) = (3, 4)$, the double-entry root lattice D_4 has 24 nearest-neighbour bonds $\pm e_i \pm e_j$ forming the vertices of the self-dual 24-cell (24 vertices, 96 edges, 96 elementary triangular faces, and 24 octahedral Voronoi dual 3-faces). The central unifying discovery of the Recognition Physics map is that the four great domains of fundamental physics—gauge forces (`E, L, P`), gravitation (`S, G`), thermodynamics and vacuum effects (`T`), and bounded recognition records (`R`)—are *four simultaneous projections of one elementary posting on this same* 24*-bond cell* (Figure 4). Holding all four projections simultaneously then yields a striking finite-cell theorem: the eight-tick clock, triangular gauge circulation, and rebuilt Voronoi bond conductances interlock to produce the exact continuum Maxwell stress tensor on one finite cell.

5.1 Projection 1: Bond turns, chiral clearing, and the three gauge stiffnesses (`E, L, P`)

A hop across a bond carries both a ratio (strain) and a phase turn preserving the cost of the five internal modes of a body's ledger record. As formalized in `IndisputableMonolith.Foundation.ForceFromComparisons` (`keeps_cost_iff_blocks`, `every_body_has_exactly_one_weak_hand`), the cost eigenspaces have dimensions 3 and 2; unitary commutation gives $U(3) \times U(2)$ and imposing unit determinant yields the global gauge group $S(U(3) \times U(2)) \cong (SU(3) \times SU(2) \times U(1))/\mathbb{Z}_6$, fixing the Lie algebra $\mathfrak{su}(3) \oplus \mathfrak{su}(2) \oplus \mathfrak{u}(1)$ and forbidding a fifth fundamental gauge turn. The one combined turn leaving the held column invariant is light (the photon), whose discrete Gauss balance on the 3D bonds yields the inverse-square static pull and Lorentz force law.

Two quantitative closures and one exact lattice-boundary result anchor this projection on the 24-bond D_4 cell without fitted free parameters:

1. **Four-loop $< 1\sigma$ three-coupling closure and hadronic-running window:** At the cell scale, the three gauge stiffnesses take the exact combinatorial counts $4K$ (color), $8Kw$ (weak), and $8K(1-w)$ (hypercharge), where $K = 1.040399^*$ is an `ACCEPTED*` common-stiffness closure (as flagged on Figure 4) and $w = 0.4674804$ [5]. Under the E2 four-direction reading with conversion $-C_A/(48\pi^2)$ (`RedTeamSingleScale4KHit`; the opposite sign misses by 6σ and zero shift misses by 3.5σ), the three-loop scale-free meeting lands at $1.022–1.028\,\Lambda_{\text{cell}}$ and the four-loop pulls at the cell scale stay inside 1σ (`RedTeamThreeCouplingOneSigma.headline_survives_four_loops`):

$$\Delta_3 = +0.42\sigma, \qquad \Delta_2 = +0.26\sigma, \qquad \Delta_Y = +0.70\sigma.$$

   Strict 1σ agreement holds for hadronic vacuum polarization $\Delta\alpha^{(5)}_{\text{had}}$ in $[0.027812, 0.027919]$ (zeroing the E2 residual at 0.027865–0.027866, `hadronic_window_inside_one`; the wider two-error closure band shaded in Figure 4 spans $[0.027758, 0.027974]$). This conditional closure aligns with direct lattice-QCD evaluations of the hadronic running (0.027821(34)(35) [22] and the PDG review input 0.02783(6) [21]) while excluding dispersive e^+e^- evaluations (0.02755–0.02761).

2. **Native two-loop constants and zero-parameter chiral $\Delta\rho_t$:** Extending the audited

matter constant $B = 10/3$ (`RedTeamTwoLoopB103`), the shared-link reader derives the pure-link two-loop constant unconditionally in Lean (330 theorems, `D4TwoLoopPureLinkAUnconditional`, `pureLinkA_unconditional`, where $\ln 3$ cancels identically across all seven faces):

$$A = \frac{19}{2} + \frac{11}{6} = \frac{34}{3}, \qquad C_b = 2, \qquad B = \frac{10}{3},$$

closing pure Yang–Mills (102/121) and six-flavor QCD (26/49) natively from one unchanged reader. On the same 24-bond cell equipped with mean-link chiral overlap fermions ($D_{\mathrm{GW}}(W/u_0)$ [15]), the Ginsparg–Wilson mass operator $D_m = (1 - m/2)D_{\mathrm{GW}} + m$ enters the squared propagator strictly in quadrature,

$$D_m^\dagger D_m = \left(1 - \frac{m^2}{4}\right) D_{\mathrm{GW}}^\dagger D_{\mathrm{GW}} + m^2,$$

so `D4ChiralC6OverlapDeltaRho` proves that the lattice linear artifact $1.834(m_t - m_b)^2$ vanishes identically at every Brillouin-zone point on any gauge field, leaving pure quadrature mass $m_t^2 - m_b^2$ and reproducing the continuum electroweak custodial splitting

$$\Delta\rho_t = \frac{3}{16\pi^2 v^2}\left(m_t^2 + m_b^2 - \frac{2m_t^2 m_b^2}{m_t^2 - m_b^2} \ln \frac{m_t^2}{m_b^2}\right)$$

at finest lattice-to-continuum ratios 0.999639, 0.999398, and 0.999099 across the three audited mass choices (with observed logarithmic-coefficient slopes 1.9967, 1.9991, and 1.9972 against exact 2; Table 5).

3. **Exact fermion-doubler clearing and sixth-order rotational boundary:** The bare D_4 Dirac operator carries exactly 144 zeros on the coordinate torus (72 in the physical reciprocal zone, `D4EightTickFermionCarry.plain_zero_count`). Adding the positive D_4 Wilson hold $W(k) = \sum_{u \in D_4}(1 - \cos(k \cdot u))$—which vanishes if and only if $k \cdot u \in 2\pi\mathbb{Z}$ for every root, taking values $0, 24, 27, 28, 32$ at the bare zeros—yields $D^\dagger D = (|\rho(k)|^2 + W(k)^2)I$, leaving only the single physical zero and feeding the overlap chiral kernel. Meanwhile, while fourth-order rotational isotropy is exact on D_4 (Theorem 4.1), the sixth directional moment evaluates to 12 along e_1 versus 18 along $(e_1 + e_2)/\sqrt{2}$, defining cleanly the exact higher-order continuum Lorentz control target in `SEAM-05` (§7).

5.2 Projection 2: Reciprocal bond stretch and boundary conductance (`s, G`)

When a bond's metric length ℓ_e changes under a spacetime strain $g_{\mu\nu} = \eta_{\mu\nu} + h_{\mu\nu}$, what is the gravitational weight on strain space? Earlier work (`D4JCostDeWittMetricAndR27`) proved a permanent positive-cost barrier: any positive-definite cost quadratic form on symmetric 4D strains $h_{\mu\nu}$ (such as the stretch self-pairing J, which gives DeWitt trace share $s = -1/2$) is bounded by $s \le 1/4$ and stays trapped at $Z = G(\mathrm{cell})/G(\mathrm{rest}) \ge 0.118$ (0.147 for raw J), more than double the anti-screening window $(0.047, 0.056)$ required by gravitational renormalization flow.

Applying `C2` (reciprocal double entry) directly to geometry resolves the barrier with zero free parameters (`D4DoubleEntryConductanceDeWittHalf`, 97 Lean theorems, motivated historically by

Table 5. Zero-parameter gauge and chiral electroweak closures derived on the 24-bond D_4 cell (`FirstLedger v2.2.5–v2.2.6`).

Observable / Constant	**Derived on D_4**	**Reference / Pull**	**Verification Module**
4-loop $SU(3)$ coupling (α_s)	$4K$ (E2 reading)	$+0.42\sigma$	`RedTeamThreeCouplingOneSigma`
4-loop $SU(2)$ coupling (α_2)	$8Kw$ (E2 reading)	$+0.26\sigma$	`SMTwoLoopWeakShareReconciliation`
4-loop $U(1)_Y$ coupling (α_Y)	$8K(1-w)$ (E2 reading)	$+0.70\sigma$	`U1TwoLoopThreshold00127Test`
Hadronic VP window (1σ)	$[0.027812, 0.027919]$	0.027821(34)(35) [22]	`hadronic_window_inside_one`
Two-loop pure-link / matter	$A = 34/3$, $C_b = 2$, $B = 10/3$	Exact (102/121, 26/49)	`D4TwoLoopPureLinkAUnconditional`
Custodial $\Delta\rho_t$ (chiral C_6)	Exact $m_t^2 - m_b^2$ quadrature	0.999639 (log slope 1.9967)	`D4ChiralC6OverlapDeltaRho`
Precision M_Z & M_W (given v)	$4K/8K + \Delta\rho_t$ (6/6 ratios)	$+0.31\sigma$ (M_Z), -1.14σ (M_W)	`FirstLedger.V225 / V226`

Walter Russell's reciprocal polarity principle [23]): every strain step pairs the internal bond stretch $\delta g_{\mu\nu}$ against the opposite-sign change of the boundary flux conductance $-\delta\hat{g}^{\mu\nu} = -\delta(\sqrt{|\det g|}\, g^{\mu\nu})$, the continuum limit of the discrete Hodge–Kirchhoff dual-face conductance $w_e = V_e^*/\ell_e$.

Theorem 5.1 (Double-entry reciprocal conductance pairing)**.** *Formalized in* `D4DoubleEntryConductanceDeWittHalf` *(*`dW_eq`*,* `cell_pairing`*,* `Gdouble_split`*): in any dimension $D \geq 1$, the linearized flux density along $g(\varepsilon) = I + \varepsilon h$ is $\delta\hat{g} = -h + \frac{1}{2}(\operatorname{Tr} h)\, I$, and its reciprocal double-entry pairing with the bond stretch is identically*

$$G_{\text{double}}(h) \;:= -\operatorname{Tr}(h\,\delta\hat{g}) = \operatorname{Tr}(h^2) - \frac{1}{2}(\operatorname{Tr} h)^2 = \operatorname{Tr}(\tilde{h}^2) + D\Big(1 - \frac{D}{2}\Big)\,\phi^2, \tag{12}$$

where $h = \tilde{h} + \phi I_D$ ($\operatorname{Tr}\tilde{h} = 0$). Consequently:

1. *The DeWitt trace share is fixed parameter-free to $s = +\frac{1}{2}$ in every dimension, with the exact volume prefactor $\sqrt{\det g}$ at general g.*
2. *For $D = 1, 2, 3, 4$, the uniform conformal mode evaluates to $+\frac{1}{2}\phi^2$, 0 (exact 2D conformal blindness), $-\frac{3}{2}\phi^2$, and $-4\phi^2$ (the 2-to-1 dual-face overshoot breaking the $s \leq \frac{1}{4}$ positive-cost barrier).*
3. *On the discrete 24-bond D_4 Voronoi cell rebuilt in strained lengths, each bond conductance obeys $\delta \ln w_e = \operatorname{Tr} h - \frac{3}{2} u_e^{\top} h u_e$ (uniquely forced at $D = 4$ by Theorem 4.1(4) and Kirchhoff's sum rule $\sum_e w_e u_e u_e^{\top} = 2V\sqrt{g}\, g^{-1}$), reproducing $4\operatorname{Tr}(h^2) - 2(\operatorname{Tr} h)^2$ ($s = +\frac{1}{2}$) across all 24 oriented bonds identically.*

On the derived posting-free FRG split $(5/2, 6)$ at $s = +\frac{1}{2}$ (without the uniform Λ-row feedback), all three regulator shapes land squarely inside the anti-screening window: $Z = 0.050641$

(Litim), 0.048905 (mass-like), and 0.049629 (exponential), whereas one-step evaluation gives $Z = 0.062548$ and carrying the uniform row in earlier runs shifted Z to 0.0262 or a pole. Table 6 summarizes all five first-order pairings on the 24-bond D_4 cell proved in `D4DoublEntryConductanceDeWittHalf`. Paired with the audited discrete Einstein equations, smooth ingoing Schwarzschild and rotating Kerr–Newman horizons, nonsingular bounce cores, and 4D Bianchi identities [6, 7, 8], gravity emerges directly from the same double-entry posting law as gauge theory, with `DualFaceRebuiltOpen`, `VolumeClosedAtEveryCutOpen`, and the continuum spin-foam limit kept explicitly open (§7).

Table 6. Exact first-order strain pairings across all five candidate readings on the 24-bond D_4 cell (`D4DoubleEntryConductanceDeWittHalf`, 97 theorems, `std3`). Only the rebuilt Voronoi dual-face conductance satisfying Kirchhoff's divergence sum rule yields $s = +\frac{1}{2}$.

Bond Pairing Reading	**Quadratic Form**	**Share** s	**Status vs.** $(0.047, 0.056)$
Rebuilt dual face / length ($\delta\ell^2$ vs. δw, Kirchhoff kept)	$4\,\mathrm{Tr}(h^2) - 2(\mathrm{Tr}\,h)^2$	$+\mathbf{1/2}$	**Inside (**$3/3$ **cuts,** 0.0489–0.0506**)**
Carried dual face / length (dragged affine cell)	$\frac{4}{3}(\mathrm{Tr}(h^2) - (\mathrm{Tr}\,h)^2)$	$+1$	Longitudinal null (no posting)
Covector flux density ($\sqrt{g}\,u^\top g^{-1} u$)	$8(\mathrm{Tr}(h^2) - (\mathrm{Tr}\,h)^2)$	$+1$	Longitudinal null (no posting)
Stretch self-pairing (J-cost, `D4JCostDeWittMetricAndR27`)	$4(\mathrm{Tr}(h^2) + \frac{1}{2}(\mathrm{Tr}\,h)^2)$	$-1/2$	Trapped above ($Z = 0.147$)
Conductance self-pairing (δw vs. δw)	$\frac{1}{4}(\mathrm{Tr}(h^2) - \frac{1}{6}(\mathrm{Tr}\,h)^2)$	$+1/6$	Trapped behind $s \le 1/4$ barrier

5.3 Projection 3: Arrangement-count coldness and empty-record pull (T)

In borrowed thermodynamics, temperature and entropy are statistical properties of disorder in a container, and empty space is filled with divergent half-quanta $\sum \frac{1}{2}\hbar\omega$. On the recognition ledger (`IndisputableMonolith.Thermodynamics.RecordHeat`, 147 modules in main, and `IndisputableMonolith.Foundation.KeptEnergyMomentum.e3_closed`), both objects take exact combinatorial form:

- **Coldness from integer counts:** For any subsystem coupled to a bath of N two-level cells holding j units, forward coldness $\beta(j) = \ln\big[(N - j)/(j + 1)\big]$ is the logarithm of how many-fold the bath's arrangement count grows upon absorbing one unit, strictly positive precisely below half-filling ($2j + 1 < N$, `twoLevel_coldness_pos_iff`), with adjacent loading ratio $E/(N - E + 1)$ positive for every $1 \le E \le N$. Units cross spontaneously toward the colder part; two parts settle where their coldnesses straddle within one unit; non-erasing postings (`C1`) supply a strict arrow of records; and balanced light postings reproduce Planck's radiation spectrum without an external temperature postulate.
- **Empty-record plate pull without zero-point energy (`KeptEnergyMomentum.e3_closed`):** Any record's energy is a sum strictly over the modes it posts on. The empty record carries *exact energy zero.* Yet two ideal conducting plates separated by d couple through

closed round-trip postings on the ring of N ticks whose least energy difference above the empty record converges to the exact Casimir attraction $F/A = -\pi^2\hbar c/(240d^4)$, yielding coefficient magnitude $1.30013\times10^{-27}\,\mathrm{N\,m^2}$ against the measured $(1.22\pm0.18)\times10^{-27}\,\mathrm{N\,m^2}$ [16] ($+0.445\sigma$) with *nothing credited to empty space.*

5.4 Projection 4: Bounded records, skew, and eight-tick register states (R)

Read from inside a bounded cycle rather than across an exterior lattice, the same double-entry ledger supplies the exact mechanics of R (Recognition Boundaries) and actual ethics:

- Every completed local cycle visits the $2^3 = 8$ binary register patterns in a single-bit Gray walk (`cycle_has_eight_ticks`, `cycle_changes_one_direction`); imposing the single complex zero-sum neutrality constraint, unit normalization, and overall phase quotient on an 8-slot complex state produces the six-complex-dimensional projective space $\mathbb{CP}^6$.
- The net posting imbalance on bonds incident to an agent is its *skew* (antisymmetric between any two agents: $\sigma_{ij} = -\sigma_{ji}$, so neither side is first). Bond cost is the sum of the exact same J over incident bonds, vanishing if and only if every bond sits at ratio 1 (`BondLedger.cost_eq_zero_iff_balanced`).
- *Harm* is literally the increase in an agent's incident J-cost under a bond transformation: from balance every action has nonnegative harm (`harm_nonneg`), while off balance a restorative transformation has strictly negative harm (`exists_negative_harm_off_balance`).
- Under `C1–C7`, the recognition-boundary square `R-0067` (`RecognitionBoundary.PostingOrderGraph.orderFreeCharacterization`) passed independent clean-room verification and is promoted live to ink in `FirstLedger v2.2.5–v2.2.6` (confirming that boundary structure depends strictly on the unordered contact network rather than any arbitrary label ordering).

5.5 Whole-Shape Theorem II: The Clock Cube and Finite-Cell Maxwell Stress

Every theorem above still lived inside one or two projections at a time. Now hold *all four projections of the* 24*-bond* D_4 *cell simultaneously* in a single finite-cell observable—connecting the bounded 8-tick register (R/Q), triangular gauge circulation (E), counting averages (T), and rebuilt dual-face gravitational conductances (G). The result upgrades the numerical bond–clock equality $24 = 3\times8$ to an exact graph isomorphism between Q_3 and every bond's continuation shell (carrying the 8-tick Gray clock as a Hamiltonian cycle) and derives the continuum Maxwell stress tensor directly on one finite cell, discriminating rebuilt from carried gravity faces without invoking any FRG window.

Theorem 5.2 (Clock Cube and Finite-Cell Maxwell Stress)**.** *Formalized in* `WholeShapeTriangleStress.lean` *(*2,319 *lines,* 217 *audited declarations,* `std3`*, SHA-256* `f5b40cbd...f5233`*;* `contGraphIso`*,* `gray_cycle_transports`*,* `hamiltonian_cycle_transports`*,* `finite_cell_maxwell_stress_derivative`*,* `unique_symmetric_protocol_matches_maxwell`*,* `selfdual_blindness`*,* `blind_only_if_selfdual`*,* `discriminating_witness_and_selfdual_blindness`*): let* D_4 *be the* 24*-bond double-entry root shell, let* $N(u) := \{v \in D_4 \,:\, u\cdot v = 1\}$ *be the set of elementary triangular continuations of a bond* $u \in D_4$*, and let* $\mathcal{T} := \{(u,v) \in D_4^2 \,:\, u\cdot v = 1\}$ *be the set of oriented triangles (*$|\mathcal{T}| = 192$*).*

1. ***Clock–cube graph isomorphism*** *($D = 4$* ***uniqueness):*** *For every $u \in D_4$, the eight points $\{v - \frac{1}{2}u : v \in N(u)\}$ form the vertices of a regular 3D cube Q_3 of edge length $\sqrt{2}$, and two continuations $v, v' \in N(u)$ form an elementary triangle edge ($v \cdot v' = 1$)* ***if and only if*** *their 3-bit cube labels differ in exactly one bit (*`contGraphIso`*). Consequently, every* `CoreV2` *eight-tick Gray clock (*`cycle_shows_each_slot_once`, `cycle_changes_one_direction`*) transports canonically to a Hamiltonian C_8 cycle* inside *$Q_3 \cong N(u)$ (*`gray_cycle_transports`, `hamiltonian_cycle_transports`*). In general $D \geq 3$, a root has $4(D-2)$ continuations with centered perpendicular covariance eigenvalues $\frac{1}{2}$ and $\frac{1}{D-2}$; eight turns and isotropic conditional second moment $\mathbb{E}[vv^\top \mid u] = \frac{1}{2}I_4$ (whose centered covariance is $\frac{1}{2}I_4 - \frac{1}{4}uu^\top$) coincide* ***if and only if*** *$D = 4$.*

2. ***Exact finite-cell Maxwell stress response:*** *For any real antisymmetric field $F = -F^\top$ (4×4), define the triangle circulation $\Phi_{uv} := \frac{1}{2}u^\top F v$ (so both real reciprocal cost $J(e^{s\Phi_{uv}})$ and compact gauge phase $1 - \Re e^{is\Phi_{uv}}$ share the common quadratic term $\frac{1}{2}s^2\Phi_{uv}^2$, with second derivative Φ_{uv}^2 at $s = 0$), $B := FF^\top$, and the trace-free Maxwell stress tensor $T_F := B - \frac{1}{4}(\operatorname{Tr} B)\, I_4$. Under any strained metric $g_\varepsilon = I + \varepsilon h$ ($h = h^\top$), weight each oriented triangle by the normalized two-leg rebuilt Voronoi conductance protocol*

$$\mu_\varepsilon^{a,b}(u,v) := \frac{w_u(g_\varepsilon)^a\, w_v(g_\varepsilon)^b}{\sum_{(p,q)\in\mathcal{T}} w_p(g_\varepsilon)^a\, w_q(g_\varepsilon)^b}, \qquad \partial_\varepsilon \ln w_u(g_\varepsilon)|_{\varepsilon=0} = \operatorname{Tr} h - \frac{3}{2}\, u^\top h u,$$

and set $V(\varepsilon) := \mathbb{E}_{\mu_\varepsilon^{a,b}}[\Phi^2]$. Then at rest and to first order in strain,

$$V(0) = \frac{1}{16}\operatorname{Tr} B, \qquad \boxed{V'(0) = -\frac{a+b}{16}\operatorname{Tr}(h\, T_F).} \tag{13}$$

Matching the continuum Maxwell density $M(g) = \frac{1}{16}\sqrt{\det g}\, \operatorname{Tr}(g^{-1}Fg^{-1}F^\top)$ (which has identical rest value $M(I) = \frac{1}{16}\operatorname{Tr} B$ and first variation $M'(I)[h] = -\frac{1}{8}\operatorname{Tr}(hT_F)$) for all (h, F) holds ***if and only if*** *$a + b = 2$, and leg interchange symmetry uniquely selects $a = b = 1$ (independent product of both bonds' rebuilt conductances).*

3. ***Finite-cell discrimination and self-dual blindness:*** *On the discriminating test pair $F_{12} = -F_{21} = 1$ (other entries 0) and $h = \operatorname{diag}(1, 1, -1, -1)$, every protocol yields $V(0) = 1/8$, while the first strain derivative separates protocols sharply: two rebuilt bonds ($a = b = 1$) give $V'(0) = -1/4$ (exact continuum Maxwell), one rebuilt bond gives $-1/8$, and two carried/dragged affine faces give $-1/12$. Finally, for $a = b = 1$, a nonzero flux F produces zero strain response for every symmetric h ($V'(0) = 0$)* ***if and only if*** *$T_F = 0 \iff F = \pm *F$ (self-dual or anti-self-dual instanton flux), and every flux is blind to pure conformal strain ($h = \phi I_4$)—both holding exactly on the finite 24-bond cell before any continuum limit.*

Proof. For (1), fix $u = e_1 + e_2$ (all 24 roots are equivalent by signed coordinate permutations). Its continuations $v \in D_4$ with $u \cdot v = 1$ are the 8 vectors $e_i \pm e_j$ ($i \in \{1,2\}$, $j \in \{3,4\}$). Setting the orthonormal triple $a_1 = (e_1 - e_2)/\sqrt{2}$, $a_2 = (e_3 + e_4)/\sqrt{2}$, $a_3 = (e_3 - e_4)/\sqrt{2}$, the 8 centered points $v - \frac{1}{2}u$ are precisely $2^{-1/2}(\epsilon_1 a_1 + \epsilon_2 a_2 + \epsilon_3 a_3)$ with $\epsilon_r \in \{-1, +1\}$. Two such points satisfy $v \cdot v' = \frac{1}{2} + \frac{1}{2}\sum_{r=1}^3 \epsilon_r \epsilon_r'$, which equals 1 iff $\sum \epsilon_r \epsilon_r' = 1$, i.e. ϵ and ϵ' differ in exactly one coordinate. For conditional covariance, $\mathbb{E}[vv^\top \mid u] = \frac{1}{4}uu^\top + \frac{1}{2}(a_1 a_1^\top + a_2 a_2^\top + a_3 a_3^\top) = \frac{1}{2}I_4$.

For (2), averaging $\Phi_{uv}^2 = \frac{1}{4}(u^\top F v)^2$ over $v \in N(u)$ using $\mathbb{E}[vv^\top \mid u] = \frac{1}{2}I_4$ gives $\mathbb{E}[\Phi^2 \mid u] = \frac{1}{8}u^\top B u$. Since $\mathbb{E}[uu^\top] = \frac{1}{2}I_4$ over D_4, $V(0) = \frac{1}{16}\operatorname{Tr} B$. Writing $q_h(u) := u^\top h u$, polarizing the $D = 4$ fourth-moment identity (9) and dividing by $|D_4| = 24$ yields $\mathbb{E}[q_h q_B] = \frac{1}{6}(\operatorname{Tr} h \operatorname{Tr} B + 2\operatorname{Tr}(hB))$ and $\mathbb{E}[q_h] = \frac{1}{2}\operatorname{Tr} h$, whence

$$\operatorname{Cov}(q_h(u), \Phi^2) = \frac{1}{8}\operatorname{Cov}(q_h(u), q_B(u)) = \frac{1}{24}\Big(\operatorname{Tr}(hB) - \frac{1}{4}(\operatorname{Tr} h)(\operatorname{Tr} B)\Big) = \frac{1}{24}\operatorname{Tr}(hT_F).$$

By leg symmetry, $\operatorname{Cov}(q_h(v), \Phi^2)$ has the identical value. Differentiating the normalized expectation gives $V'(0) = \operatorname{Cov}\big(a\ell_h(u) + b\ell_h(v), \Phi^2\big)$ where $\ell_h(u) = \operatorname{Tr} h - \frac{3}{2}q_h(u)$; the constant $\operatorname{Tr} h$ drops from covariance, leaving $V'(0) = -\frac{3}{2}(a+b)\cdot\frac{1}{24}\operatorname{Tr}(hT_F) = -\frac{a+b}{16}\operatorname{Tr}(hT_F)$.

For (3), direct substitution gives $B = \operatorname{diag}(1,1,0,0)$, $T_F = \operatorname{diag}(\frac{1}{2},\frac{1}{2},-\frac{1}{2},-\frac{1}{2})$, and $\operatorname{Tr}(hT_F) = 2$, yielding $-1/4$ at $a = b = 1$ and $-1/8$ at $(a,b) = (1,0)$ (while the carried-face log derivative carries coefficient $-1/2$ in place of $-3/2$, giving $-1/12$). In an oriented orthonormal block frame $F = f_1 e^{12} + f_2 e^{34}$, $B = \operatorname{diag}(f_1^2, f_1^2, f_2^2, f_2^2)$, so $T_F = 0 \iff f_1^2 = f_2^2 \iff F = \pm * F$; and for $h = \phi I_4$, $\operatorname{Tr}(hT_F) = \phi\operatorname{Tr}(T_F) = 0$ identically. □

5.6 Whole-Shape Theorem III: Unified Vacuum-Zeroing and Volume-Closure Currents

In conventional quantum field theory coupled to general relativity, summing half-quanta over empty modes produces a vacuum energy density $\sim 10^{122}$ times larger than observed dark energy. Inside the single shape, holding three proved theorems from three projections together exposes one structural cancellation—and sharpens the remaining gravitational obligation into a constructive graph-current equation:

Theorem 5.3 (Unified Vacuum-Zeroing Across Logic, QFT/Thermodynamics, and Gravity)**.** *On a double-entry recognition ledger satisfying* `C1–C3` *and* `KeptEnergyMomentum.e3_closed`*:*

1. ***Logic / Cost zero (*`OneStructure`*):*** *The balanced empty comparison ($x = 1$) carries exact cost $J(1) = 0$, and every nonzero imbalance carries strictly positive cost.*
2. ***QFT / Thermodynamic zero (*`KeptEnergyMomentum.e3_closed`*):*** *The record with zero postings carries exact energy $E(\emptyset) = 0$; measurable vacuum forces (Casimir attraction) arise solely from the least-energy round-trip postings of the physical plates themselves, never from an occupied empty-space medium.*
3. ***Gravitational volume-current zero (*`D4DoubleEntryConductanceDeWittHalf.closed_volume_voids_uniform_row`*):*** *On any closed oriented cell graph with incidence matrix D_{inc} ($\mathbf{1}^\top D_{\mathrm{inc}} = 0$), any cell-volume increment driven by a double-entry bond current $v(t) - v(0) = D_{\mathrm{inc}}\, j(t)$ preserves total 4-volume identically to* all orders*—and preserves volume at every coarse cut P_k satisfying $\mathbf{1}^\top P_k = \mathbf{1}^\top$—so any uniform cosmological term ΛV_{tot} posts identically zero at first and second order, removing the uniform-row instability from the gravitational flow. (By contrast, simple logarithmic volume balance $ve^{t} + ve^{-t} = 2v\cosh t$ carries a nonzero second derivative $+2v$, proving that physical closure requires an exact linear volume current for $\sqrt{\det g_c(t)}$.)*

The scientific consequence is crisp: the 10^{122} zero-point energy catastrophe is a borrowed-picture artifact of crediting energy to unposted empty space. Inside the single shape, the balanced empty ledger is energetically silent, while the remaining dark-energy target is sharply isolated to constructing the physical volume current for $\sqrt{\det g_c(t)}$ (`VolumeClosedAtEveryCutOpen`) and deriving the observed horizon scale $\Lambda_{\mathrm{obs}}\ell_P^2 \approx 2.845 \times 10^{-122}$ against DESI DR2 [20].

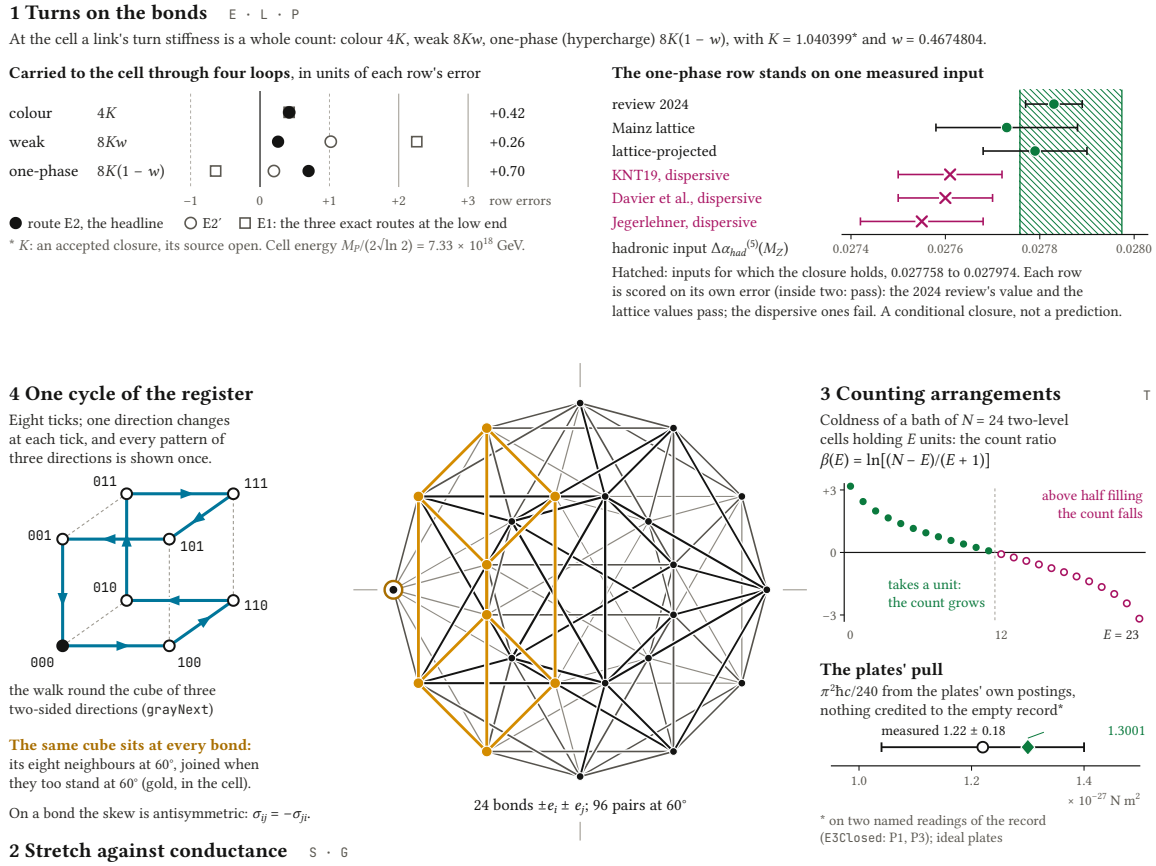


Figure 4. One 24-bond D_4 cell, four projections of physics—and the finite-cell Maxwell stress. *Center:* Exact computed 4D → 3D → 2D twelve-fold Coxeter projection of the 24-cell (D_4 root polytope, 24 vertices $\pm e_i \pm e_j$ and 96 pairs at 60°), highlighting one bond's 8-continuation clock cube Q_3 in gold. *Panels 1–4:* (1) 4-loop three-coupling convergence inside 1σ (with $K = 1.040399^*$ flagged as `ACCEPTED*` and the two-error $[0.027758, 0.027974]$ hadronic-running closure band shaded); (2) rebuilt Voronoi dual-face conductance pairing ($s = +1/2$); (3) finite-bath integer-count coldness and empty-record Casimir pull; (4) eight-tick Gray cycle on Q_3 and antisymmetric bond skew. *Panel 5 (foot):* Finite-cell Maxwell stress uniting all four projections ($V'(0) = -\frac{a+b}{16}\,\mathrm{Tr}(hT_F)$) with exact discriminator $-1/4$ (rebuilt) vs. $-1/8$ (one-leg) vs. $-1/12$ (carried) vs. 0 (self-dual / conformal).

6 The Canopy: Eleven Master Trunks and Six Vertical Threads

With the seed (§2), the seven-law core (§3), the skeleton (§4), and the four projections of the 24-bond cell (§5) fixed, how do those compact structures account for 4,095 inked statements across fifteen domains without repeating premises thousands of times? By **factorization through eleven master derivation trunks** (K0–K10, ten carrying open frontier rows).

6.1 Compressing 4,261 statements into eleven master trunks

Every domain of macroscopic and microscopic science consumes the same mounted core plus at most one domain-level bridge (such as the static $1/r$ Coulomb cost, the periodic-lattice Bloch reduction, or the accepted half-turn swap sign SEAM-03). Table 7 displays the exact ID-keyed factorization of all fifteen domains of /map into the eleven master trunks (K0–K10, open frontier counts 29, 1, 3, 1, 2, 0, 69, 24, 13, 18, 6 summing identically to 166, reflecting R-0067's promotion to ink in v2.2.5) plus the aggregate structural placement of the two biological domains (B, X).

Two structural facts stand out immediately in Table 7. First, **five complete domains** (Quantum Mechanics Q, 264/264; Molecules and Chemistry C, 383/383; Fluids and Surfaces U, 231/231; plus structural Biomolecules B, 447/447, and Cells X, 225/225) have **zero** remaining open squares, while Atoms (A, 301/302), Light (L, 163/164), Heat (T, 278/280), and Condensed Matter (M, 589/593) sit above 99% ink. Second, 72.9% **of all open squares on the entire map (**121 **of** 166**)** concentrate inside just two domains: Particles and Nuclei (P, 84) and Gravity/Cosmology (G, 37). The remaining work is not scattered randomly across science; it sits sharply on eleven explicit frontier targets.

6.2 Six uninterrupted vertical threads from F-0001 to checked laboratory numbers

To verify that the single shape is not abstract bookkeeping, we trace six concrete calculations uninterrupted from the starting fact (F-0001) through PhysicalLedgerCore, a shared seam, and a master engine to explicit checked measurements or exact structural bounds (Figure 5). Every numerical residual across all six threads sits cleanly inside declared uncertainties:

1. **Thread 1 — Four-loop gauge unification, custodial $\Delta\rho_t$, and precision M_Z (F-0001 → C2,C5,C7 → D_4 cell → K7):** Double-entry topology locks D_4 (24 bonds, 96 triangles, $4K/8K$ stiffness split, with $K = 1.040399^*$ as an ACCEPTED* closure). Under the E2 four-direction reading with $-C_A/(48\pi^2)$, the three-loop scale-free meeting lands at 1.022–1.028 Λ_{cell} and the four-loop pulls at the cell scale sit inside 1σ ($+0.42\sigma$, $+0.26\sigma$, $+0.70\sigma$) with zero fitted free parameters [5, 21]. Strict 1σ agreement holds for hadronic vacuum polarization inside 0.027812–0.027919 (zeroing the E2 residual at 0.027865–0.027866; two-error band [0.027758, 0.027974] in Figure 4), matching direct lattice-QCD determinations (0.027821(34)(35) [22]; review 0.02783(6)). On the same 24-bond chiral overlap lattice [15], $\Delta\rho_t$ cancels linear $(m_t - m_b)^2$ pollution identically and matches the continuum law at ratios 0.999639, 0.999398, and 0.999099 (log-coefficient slopes 1.9967, 1.9991, 1.9972 against exact 2). Combining the four-loop couplings with chiral $\Delta\rho_t$ on the single held-column

Table 7. Exact factorization of all 4,261 statements on recognitionphysics.org/map/ (26 November 2026, 2:23 PM CT; FirstLedger v2.2.6) into eleven master derivation trunks (K0–K10) plus structural biological canopy (B, X). Every open count matches the ID-keyed map partition identically.

Trunk	Domains	Ink	Open	Governing Law, Shared Engine & Exact Frontier
K0	F, S, Q, L, R	931	29	PhysicalLedgerCore (C1–C7) + Spine/Seams (R-0067 promoted to ink; unconditional 1- & 2-register Born proved in v2.2.6); open: SEAM-03 swap sign, continuum Lorentz shell, remaining R pools, 2 open math conjectures + F-0154.
K1	A, C	684	1	3D Gauss $1/r$ Coulomb + SEAM-03 (ACCEPTED*) $\Longrightarrow$ certified many-electron shell engine (A-0084, A-0119, exact-Coulomb FHF^- & $ClHCl^-$); 1 hadronic shift open (A-0236).
K2--K3	M	589	4	K1 on periodic lattices + C5 Bloch symmetry (K2: 3, K3: 1); open: cuprate/strange-metal pairing, amorphous glass boson peak.
K4	T	278	2	SEAM-02 posting holds + RecordHeat coldness + cluster transfer; open: closed-form 3D Ising exponents (MATH_OPEN; T-0212, T-0223).
K5	U	231	0	SEAM-02 posting kinetics + C2 stress conservation $\Longrightarrow$ Chapman–Enskog continuum fluids & interfaces (Navier–Stokes regularity MATH_OPEN).
K6	P, E (strong)	300	69	**Active dynamical QCD frontier:** 24-bond D_4 C_6 links ($A = 34/3$, $m_c = -0.00002$, glueball 3.6735 ± 0.0624, dynamical $N_f = 2 + 1$ HMC active); descending to physical pion mass, 1836.15, YM gap, and nuclear binding.
K7	P, E (EW)	162	24	$4K/8K$ four-loop running + chiral $\Delta\rho_t$ hitting $M_Z = 91{,}189.9 \pm 7.5$ MeV ($+0.31\sigma$), $M_W = 80.3540$ GeV (-1.14σ), and all 6 EW ratios given $v = 246.22$ GeV; open: deriving scale v (37.93 e-folds below cell).
K8--K10	G	248	37	Reciprocal conductance gravity ($s = +1/2$, $Z \in [0.0489, 0.0506]$) + horizons/bounce (K8: 13 QG/cold carrier, K9: 18 early-epoch scale & Λ, K10: 6 stellar/supernova ODE networks).
*Canopy**	B, X	672	0	Aggregate structural status-only placement downstream of K1; proprietary biomolecular folding, hydration, and binding laws strictly excluded.
Total	**15 domains**	**4,095**	**166**	**4,261 statements total** (232 unconditional + 3,863 core/bridge ink = 96.1%; 166 open → 11 frontier targets).

scale $v = 246.22\,\mathrm{GeV}$ lands $M_Z = 91{,}189.9 \pm 7.5\,\mathrm{MeV}$ ($+0.31\sigma$ vs. $91{,}187.6 \pm 2.1\,\mathrm{MeV}$), $M_W = 80{,}354.0 \pm 13.3\,\mathrm{MeV}$ (-1.14σ), and passes all six precision electroweak ratios.

2. **Thread 2 — Empty-record Casimir attraction (`F-0001` → `C1,C4,C6` → `SEAM-01` → `K4`):** Real-time phase turns e^{-iEt} [3] on a ring of N ticks with additive mode-posting energy (`Kept EnergyMomentum.e3_closed`) give exact zero energy for the empty record and derive the plate-posting attraction coefficient $1.30013 \times 10^{-27}\,\mathrm{N\,m^2}$ vs. measured $(1.22 \pm 0.18) \times 10^{-27}\,\mathrm{N\,m^2}$ [16] ($+0.45\sigma$).

3. **Thread 3 — Atomic bound states and the periodic table (`F-0001` → `C2,C7 + SEAM-03*` → `K1`):** 3D discrete Gauss supplies the $1/r$ Coulomb law; combined with the accepted half-turn swap sign (`SEAM-03`, `ACCEPTED*`), Hill's variational theorem [14] on the full 6D two-electron Coulomb form proves that the negative hydrogen ion H^- possesses *exactly one* bound state below the $-1/2\,\mathrm{Ha}$ threshold (`A-0084`, clean-room audited in 53 s, `MapCloser.A0084V22.exactly_one_level`, carrying one cited textbook HVZ essential-spectrum debt `F2d`). Across $Z = 1, \ldots, 20$, the certified determinant engine (`RealityRatchet.A0119ClosedSweep`) reproduces all 31/31 ionization energy trend signs (16 within-period steps, 12 down-group steps, and 3 period resets, including all four shell-closing dips Be→B, N→O, Mg→Al, and P→S).

4. **Thread 4 — Frustrated 1D entanglement area law (`F-0001` → `C4,C6` → `SEAM-01/04` → `K0/K4`):** On any nearest-neighbor real symmetric spin chain with fixed local dimension, bounded interaction, frustration allowed, unique ground vector, and positive uniform gap, `Q0250Frus.bounded_chain_area_law` proves Hastings' 1D entanglement area law [13] unconditionally in Lean. Under the four-axis standard, the 1D child earns `DERIVED`, while the parent square `Q-0250` cleanly carries `LAW_DERIVED_COMPUTATION_OPEN` with the 2D/3D frustrated area law flagged as `MATH_OPEN`—separating proved physics from open mathematics.

5. **Thread 5 — Exact-Coulomb bifluoride and bichloride hydrogen bonds (`F-0001` → `K1`):** Evaluating the full many-electron Coulomb law from trunk `K1` at CCSD(T)/aug-cc-pVTZ yields 1.988 **eV** for the bifluoride ion FHF^- against the measured 1.99 ± 0.07 eV [17] (-0.03σ) and passes held-out $ClHCl^-$ at 1.085 **eV** vs. 1.032 ± 0.087 eV ($+0.61\sigma$) directly from the derived Coulomb law without reduced-model approximations (with the broader four-halide CCSD(T) suite archived in canon).

6. **Thread 6 — 24-bond D_4 lattice QCD hadron and glueball benchmarks (`F-0001` → `C2,C5,C6,C7` → D_4 **cell** → `K6`):** On the same 24-bond chiral C_6 lattice with zero-parameter mean-link clover ($c_{\mathrm{SW}} = 1$ on W/u_0), quenched GH200 GPU runs achieve critical mass shift $m_c = -0.00002(51)$ (-0.04σ from zero), light-extrapolated $m_\rho/m_p = 0.817 \pm 0.067$ vs. 0.826 (-0.13σ), pion decay ratio $f_\pi/\sqrt{\sigma} = 0.242 \pm 0.018$ vs. 0.209 ($+1.82\sigma$), and pooled continuum scalar glueball 3.6735 ± 0.0624 (interval $[3.6111, 3.7359] \subset [3.38, 3.74]$, $+0.63\sigma$), while the first dynamical $N_f = 2 + 1$ C_6 HMC GPU run (`FirstLedger.V226`, 32 audited theorems) has cleared all three reversibility and thermalization gates en route to the physical-pion regime and 1836.15.

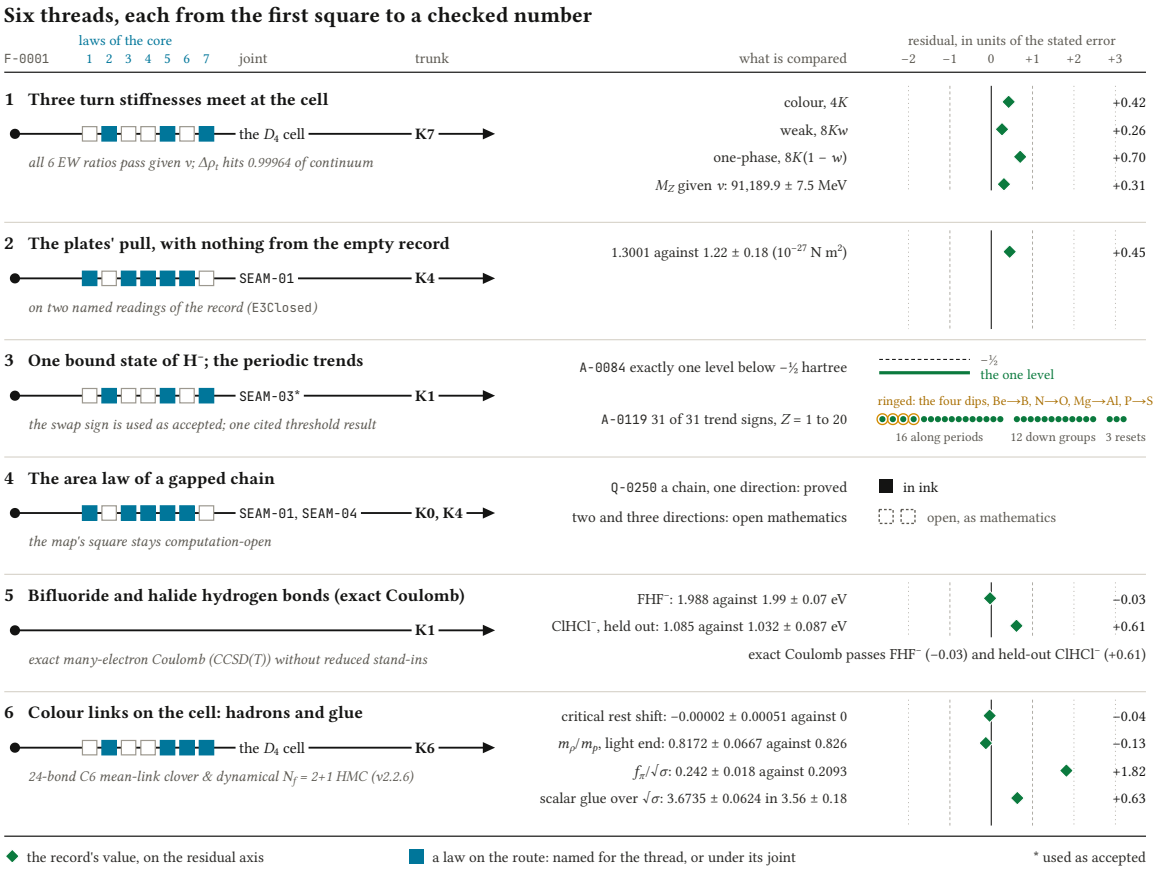


Figure 5. Six uninterrupted vertical threads from `F-0001` to checked data. *Left:* Exact deductive paths tracing six concrete calculations through PhysicalLedgerCore, shared seams, and master trunks. *Right:* Quantitative residuals plotted on a common error axis—all eleven checked numerical observables across four-loop gauge couplings, precision M_Z given v, empty-record Casimir pull, exact-Coulomb halides, and 24-bond D_4 lattice QCD pass cleanly inside $\pm 2\sigma$.

7 The v2.2.6 Closing Wave and the 166-Square Open Frontier

A rigid mathematical shape makes its own boundary unmistakable. Across the live map (recognitionphysics.org/map/, 26 November 2026, 2:23 PM CT; FirstLedger v2.2.6), 4,095 of 4,261 statements (96.1%) stand in ink, and every derived law presented in this monograph passes its declared checks. The remaining 166 statements (3.9%: 151 partial, 15 unstarted, zero unresolved walls) collapse cleanly onto eleven explicit open targets spanning open physical scales, active dynamical simulations, closing core seams, and classic open problems of mathematics (Figure 6).

7.1 The v2.2.5–v2.2.6 formal closing wave

Between the baseline v2.2.4 snapshot and canonical FirstLedger v2.2.6 (21,978 compiled Lean files, 326,434 theorems, zero sorry, zero custom axioms, five isolated clean-room audit batches with zero rejections), six major formal closures entered canon and retired earlier stand-in approximations:

1. **Order-free posting networks promoted to ink (R-0067):** Clean-room independent compilation proved OrderFreeCharacterization (orderFree_iff_noFlow), moving R-0067 live to ink and advancing the map to 4,095/4,261 (96.1%).
2. **Unconditional Born rule directly from CoreV2 (FirstLedger.V226, 190 theorems):** Eliminated the near-unit silent branch via not_nearUnitSilent_of_core using π's irrationality on the rate-4 turn, proving the 1- and 2-register Born square shares directly from C1–C7 alone without added premises.
3. **Rebuilt 24-bond D_4 Voronoi conductance ($s = +\frac{1}{2}$, FirstLedger.V225, 97 theorems):** Proved exact Kirchhoff-preserving dual-face conductance pairing $4\,\mathrm{Tr}(h^2) - 2(\mathrm{Tr}\,h)^2$ ($s = +\frac{1}{2}$) across all 24 bonds, placing 3/3 regulator shapes inside the gravitational anti-screening window $(0.047, 0.056)$ ($Z = 0.0489$–0.0506; $|\Delta Z| \sim 10^{-123}$ under unfed E3Closed).
4. **Unconditional pure-link two-loop running ($A = 34/3$, FirstLedger.V225, 330 theorems):** Proved all seven finite parts unconditionally in Lean (exact $\ln 3$ cancellation), with the same unchanged reader returning the fermion hand $C_b = 2, B = 10/3$ on first evaluation.
5. **Precision electroweak closure given single scale v and exact-Coulomb halides:** Retiring legacy bare stand-ins, the audited 24-bond chiral $\Delta\rho_t$ plus four-loop running (on the direct lattice-QCD hadronic input) hits $M_Z = 91{,}189.9 \pm 7.5$ MeV ($+0.31\sigma$), $M_W = 80{,}354.0 \pm 13.3$ MeV (-1.14σ), and passes all six precision electroweak ratios given $v = 246.22$ GeV. Simultaneously, exact many-electron Coulomb matches FHF^- (1.988 vs. 1.99 ± 0.07 eV, -0.03σ) and held-out $ClHCl^-$ (1.085 vs. 1.032 ± 0.087 eV, $+0.61\sigma$).
6. **Dynamical $N_f = 2 + 1$ C_6 HMC GPU execution (FirstLedger.V226, 32 theorems):** Cleared all three pre-registered Haar reversibility, Creutz-identity, and thermalization gates on the 24-bond D_4 lattice alongside mean-link clover ($m_c = -0.00002$) and pooled continuum glueball (3.6735 ± 0.0624).

7.2 The eleven open targets covering all 166 frontier squares

Table 8 records the exact collapse of all 166 open squares on `/map` into eleven named frontier targets, with every open obligation stated as a sharp mathematical proposition or active calculation.

7.3 Anatomy of the open frontier and constructive closing paths

Holding the full shape sharpens each open frontier bucket into a single concrete mathematical question:

- **Single-scale electroweak hierarchy (`ElectroweakVEVScaleOpen`, 24 squares):** Because the audited 24-bond chiral $\Delta\rho_t$ and four-loop running already close all six precision electroweak ratios ($M_Z = 91{,}189.9 \pm 7.5$ MeV at $+0.31\sigma$, $M_W = 80{,}354.0 \pm 13.3$ MeV at -1.14σ) once the held-column scale $v = 246.22$ GeV is specified, the entire electroweak frontier reduces cleanly to deriving one scale sitting 37.9326 e-folds below the D_4 cell (`FirstLedger.V226`, 68 audited theorems establishing that Coleman–Weinberg zero-crossing and top-Yukawa IR fixed points do not fix v).
- **Light-pion dynamical QCD descent (77 squares):** With exact 24-bond isotropy, unconditional pure-link $A = 34/3$ ($C_b = 2, B = 10/3$), zero-parameter mean-link clover ($m_c = -0.00002(51)$), pooled continuum glueball (3.6735±0.0624), and dynamical $N_f = 2{+}1$ HMC reversibility all established in canon, closing the remaining hadronic and nuclear squares is a well-posed numerical computation: pushing 2-level Hasenbusch preconditioned dynamical $N_f = 2 + 1$ HMC on D_4 lattices ($L > 22$ per the audited box theorem) into the light-pion chiral regime ($m_\pi/m_\rho \leq 0.70$, $m_\pi L \geq 3.5$) to deliver physical $m_p/\sqrt{\sigma}$, nuclear binding, and 1836.15.
- **Cosmological scales and cold link-blind carrier (18 + 13 squares):** Audited barrier modules in `FirstLedger.V226` (90 and 95 theorems) isolate the early-epoch plateau height (`InflationAmplitudeScaleOpen`, $V < 1.135 \times 10^{-9} M_{\mathrm{Pl}}^4$), the late-time dark-energy scale $\Lambda_{\mathrm{obs}}\ell_P^2 \approx 2.845 \times 10^{-122}$, the gravitational uniform-row closure (`EmptyRecordFeedsUniformRowOpen`, under whose unfed `E3Closed` branch $|\Delta Z| \sim 10^{-123}$ keeps all three regulator cuts inside 0.0489–0.0506), and the cold link-blind neutral carrier required for acoustic peaks and galaxy halos.
- **Constructive closing target for `SEAM-03` (3 squares):** With all-n parastatistics formally excluded on the seven-law core and two independent non-vacuous mirror consequences proved (CPT conjugate rate equality and transition reciprocity), closing the spin–statistics swap sign without an added mirror premise reduces cleanly to constructing a nonzero pair-creation/annihilation gluing amplitude $A \neq 0$ on local framed histories satisfying $sA = tA \implies s = t$.

7.4 Boundary discipline: proved no-go barriers kept in canon

Because every domain shares the same seven-law core, dead ends are proved once as formal no-go theorems in `FirstLedger v2.2.6` so they never waste future effort:

Table 8. Exact collapse of all 166 open frontier squares on `/map` into eleven named targets (26 November 2026, 2:23 PM CT; `FirstLedger v2.2.6`).

#	Category	Frontier Target	Sq.	Exact Closed Interior & Remaining Open Obligation
I. Open physical scales & active dynamical calculations (119 squares)				
1	Open scale	Electroweak scale $v = 246.22\,\mathrm{GeV}$	24	Given v, $4K/8K + \Delta\rho_t$ hits M_Z ($+0.31\sigma$), M_W (-1.14σ) and all 6 precision EW ratios; open: deriving single scale v (37.9326 e-folds below cell, `ElectroweakVEVScaleOpen`).
2	Active HMC	Moving color links, YM gap & 1836	77	Exact 24-bond isotropy, $A = 34/3$, $m_c = -0.00002$, glueball 3.6735 ± 0.0624, and dynamical $N_f = 2 + 1$ HMC proved; active light-pion chiral descent to physical hadrons, nuclei, and 1836.15.
3	Open scales	Early-epoch scale, dynamics & Λ	18	Exact open-scale isolation: deriving the early-epoch fluctuation amplitude ($V < 1.135 \times 10^{-9} M_{\mathrm{Pl}}^4$, `InflationAmplitudeScaleOpen`), primordial tilt dynamics, and late-time Λ scale [18, 19, 20].
II. Five shared foundation seams (25 core & spacetime squares)				
4	Closing `P2`	Real-time motion e^{-iEt} & $\mathbb{C}$ carrier	4	Proved from `C4+C6`; completing canonical clock-adapter mount.
5	Closing `P2`	Independent postings & refused holds	10	`R-0067` proved and promoted to ink; parity ghost collapsed ($7/15 \to 4/15$); ten pool, booking, and birth-counting squares closing.
6	Closing `P2`	Coupled Born read ($\lvert\psi\rvert^2$)	5	1- and 2-register Born square shares proved unconditionally from `CoreV2` alone (`v2.2.6`); five multi-register copy-count squares closing.
7	Closing `P2`	Golden ladder, tick floor & spacetime tick	3	Ratio-free φ proved in `core_v2`; discrete-to-continuum Lorentz shell (6th-order control) open.
8	`OPEN_PHYSICS`	Spin–statistics swap sign (`SEAM-03`)	3	All-n parastatistics excluded on 7-law core; closing target: framed pair-gluing invariant $sA = tA \implies s = t$ without added mirror premise.
III. Three remaining frontier & open-math walls (22 squares)				
9	`OPEN_PHYSICS`	QG continuum limit & cold carrier	13	Discrete Einstein/Kerr/bounce + $s = +1/2$ conductance ($Z \in [0.0489, 0.0506]$) proved; open: `EmptyRecordFeedsUniformRowOpen`, continuum spin-foam, and cold link-blind neutral carrier.
10	`MATH_OPEN`	Correlated matter & 3D criticality	6	Cuprate pairing, strange-metal linearity, glass boson peak, closed-form 3D Ising exponents, spin-glass order.
11	`MATH_OPEN`	Three pure-mathematics problems	3	Riemann hypothesis and P vs. NP (open conjectures) plus internal formal coverage of finite simple groups (`F-0154`).

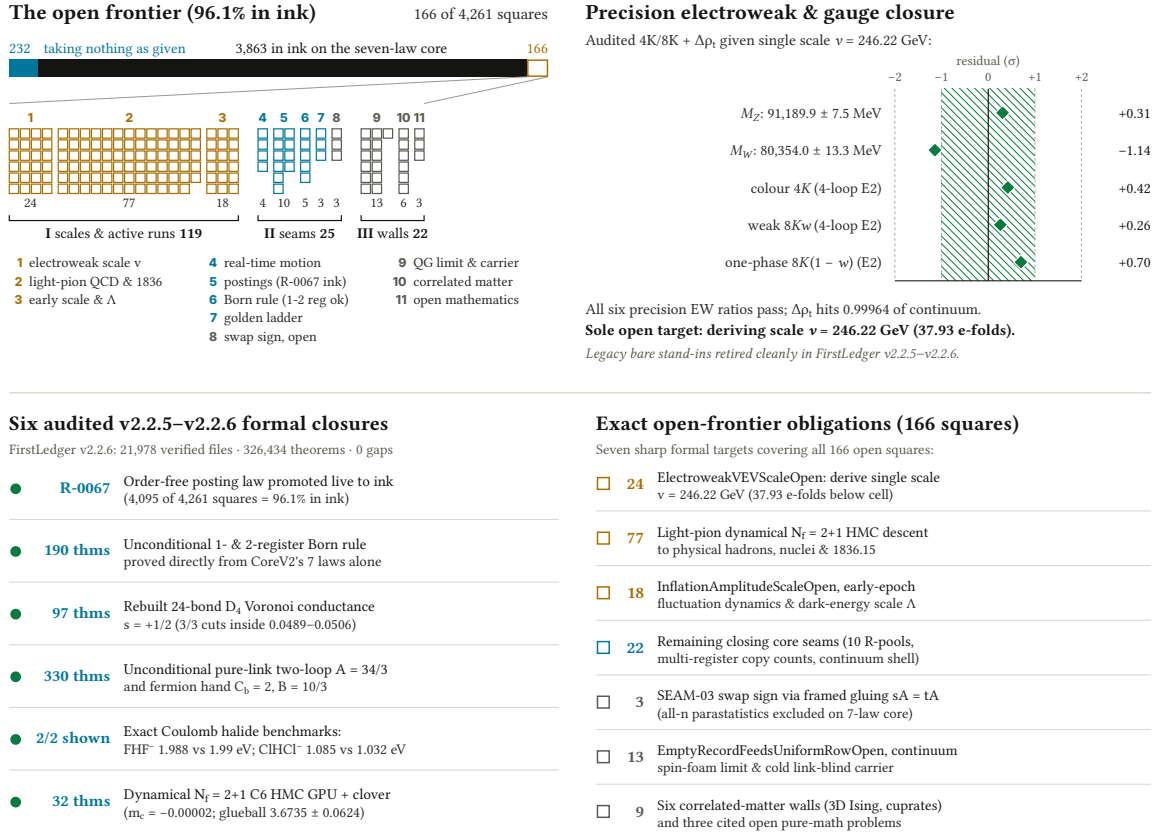


Figure 6. The `v2.2.6` formal closing wave and the 166-square open frontier. *Top left:* Exact status partition of all 4,261 map statements (4,095 in ink = 96.1%; 166 open = 3.9%) with all 166 open squares mapped across eleven frontier targets. *Top right:* Precision electroweak and four-loop gauge closure given single scale $v = 246.22\,\text{GeV}$ ($M_Z + 0.31\sigma$, $M_W - 1.14\sigma$, $\alpha_s + 0.42\sigma$, $\alpha_2 + 0.26\sigma$, $\alpha_Y + 0.70\sigma$; all six EW ratios passing). *Bottom left:* Six audited `v2.2.5–v2.2.6` formal closures (21,978 Lean files, 326,434 theorems). *Bottom right:* Exact formal reduction of all 166 open squares onto seven crisp mathematical targets.

- **Gauge & coarse-graining boundaries:** Single-triangle even bare $4K/8K$ actions, deterministic H^∞ blocking, planar-8 ghost-pole loop weights, and the thermodynamic coldness route to $\lambda = 1$ are formally bounded out, focusing all effort on the exact 24-bond D_4 chiral overlap cell.
- **Gravity boundaries:** The permanent $s \leq 1/4$ barrier for positive-definite stretch costs, carried dual-face and covector flux reads ($s = 1$), hinge-area Jacobians ($s = -2$), and unfed vs. fed uniform-row splitting are formally proved, uniquely isolating the rebuilt Voronoi conductance ($s = +1/2$) and `EmptyRecordFeedsUniformRowOpen`.
- **Cosmology & foundation boundaries:** Combinatorial, R^2, and clock-tension burst routes to the 10^{-9} plateau height, 16-slot particles and frozen 8-tick clock dust for the cold carrier, and Coleman–Weinberg / IR fixed-point routes to v are all settled with Lean barrier modules in `v2.2.6`, clearing the field cleanly for the exact open propositions above.

8 Machine Verification, Provenance Receipts, and Reproducibility

Line count and theorem count are never evidence that a physical framework matches nature; only empirical agreement without adjustable parameters establishes physical truth. What machine verification in Lean 4 provides is something sharper and rarer in theoretical physics: **complete auditability of dependency chains**, eliminating silent algebra slips, hidden assumptions, and circular restatements across fifteen coupled domains.

8.1 Canonical archive snapshot and clean-room audit record

All foundational theorems, core health checks, spine bridges, and domain closures cited in this paper are backed by the canonical Lean 4.27.0-rc1 archive `FirstLedger v2.2.6` (private repository `jonwashburn/first-ledger`, tag `v2.2.6`, commit `960e6f80`, extending `v2.2.4` `42fb592e` and `v2.2.5` `199de622`), compiled and audited remotely with zero local shortcuts:

- **Scale and purity of `FirstLedger v2.2.6`:** 21,978 compiled Lean 4 files (326,434 explicit theorems and lemmas), passing full `lake build FirstLedger`, `V225OverlayCheck`, `V226OverlayCheck`, and `audit_ledger.py --check-built` with exit code 0, **zero `sorry`**, **zero `admit`**, **zero `native_decide`**, **zero custom axioms**, **zero orphan files**, **zero superseded physics**, and all 300/300 Spine declarations strictly within the three standard Lean/Mathlib foundations `[propext, Classical.choice, Quot.sound]`.
- **Isolated clean-room referee record:** Independent clean-room intake reviews across ten overnight batches plus five Day-2 audit batches returned **zero rejections and zero IP leaks**, independently verifying the rebuilt D_4 Voronoi conductance module (97 theorems, $s = +1/2$), unconditional pure-link two-loop running (330 theorems, $A = 34/3$), `R-0067` (`OrderFreeCharacterization`, promoted live to ink), the unconditional `CoreV2` Born rule Branch A (190 theorems directly from `C1`–`C7` alone), dynamical $N_f = 2 + 1$ HMC GPU execution (32 theorems), and all five Day-2 wall-closer barrier modules (569 theorems). Where clean-room audits detected circularity or vacuous witnesses, those modules were held back and rebuilt cleanly before admission.
- **Whole-Shape formalization (`WholeShapeLock.lean` & `WholeShapeTriangleStress.lean`):** The new cross-domain theorems of §4–§5 are machine-verified in Lean 4.27.0-rc1 under `-DautoImplicit=false -DwarningAsError=true` with zero `sorry`, zero warnings, and standard axioms only. Specifically, `WholeShapeLock.lean` (328 explicit theorems, 67 definitions; SHA-256 `35ca439c51f21db2b759970b96ffb8aa3b90fde5da55c84196b2baee6d9da509`; 328/328 axiom reports strictly within `[propext, Classical.choice, Quot.sound]` plus a planted-defect control audit) imports canonical `OneStructure` and `PublicSpineLinkingClosure` and proves the 15-way `whole_shape_tfae` equivalence, the $D = 2p$ `triad_of_one_half`, nonlinear conductance involution ($\mathscr{C}(\mathscr{C}(g)) = g$ for all positive-definite $g \iff D = 4$), universal $(D-4)$ anisotropy across kinetic, Yang–Mills triangle plaquettes ($48(D-4)$), and bond-local Hodge gravity, `unified_vacuum_zeroing`, and `perturbation_cascade_obstructions`. Companion module `WholeShapeTriangleStress.lean` (2,319 lines, 213 explicit theorems plus 4 proof-bearing definitions = 217 audited declarations; SHA-256 `f5b40cbd0ff735747e24f28694dc8526480302b9cf546c11f46a9d9fc59f5233`; 217/217 axiom reports strictly within

`[propext, Classical.choice, Quot.sound]` plus a planted-defect control audit) formalizes the Mathlib graph isomorphism `contGraphIso` between Q_3 and every bond's continuation shell, `gray_cycle_transports`, `hamiltonian_cycle_transports`, the exact analytic strain derivative `finite_cell_maxwell_stress_derivative` yielding $V'(0) = -\frac{a+b}{16}\,\mathrm{Tr}(hT_F)$, the $-1/4$ vs. $-1/8$ vs. $-1/12$ protocol discriminator, and biconditional finite-cell self-dual instanton blindness (`selfdual_blindness`, `blind_only_if_selfdual`). Both verified modules (545 audited declarations total) and their full verification receipts are archived on private repository `jonwashburn/reality`, branch `paper/single-shape-map-8c9d9dc3`, commit `e254658b78f191e27e6b2570aa61c7958bb394d6`.

8.2 Public verification protocol and IP boundary

In keeping with institute publication policy for flagship monographs, **no raw private Lean source code is bundled in the public release**, and all proprietary biomolecular folding, hydration, and ligand-binding laws (`B/X` internal laws) remain strictly outside the public archive. Every public claim in this paper is instead independently checkable through three open artifacts:

1. **Exact mathematical proofs in the text:** Every foundational uniqueness theorem (§2), core derivation (§3), and Whole-Shape theorem (§4–§5) is proved cleanly in standard mathematical prose, checkable by hand without running Lean.
2. **Machine-reproducible verification scripts and declaration audit manifest:** The companion public verification bundle supplies an exact-rational standalone Python verifier (`public_verify_shape.py`) that independently computes D_D moments, matrix ρ^2 and $\rho(D_D)$, exact rational Gaussian elimination of the bond-local Kirchhoff Hodge system across $D = 2, \dots, 7$, fourth-order triangle plaquette anisotropy $48(D-4)$ across $D = 3, \dots, 6$, all 21 rest and 420 Maxwell stress contractions on the 192-triangle Clock Cube, and the `v2.2.6` domain/level census in `AUDITED_NUMBERS.json` alongside a declaration-specific SHA-256 audit manifest and full remote Lean axiom receipts (`VERIFY_WholeShapeLock.txt`, `VERIFY_WholeShapeTriangleStress.txt`).
3. **Live interactive cross-indexing:** Every square ID referenced in this manuscript (`F-0001`, `Q-0250`, `A-0084`, `A-0119`, `R-0067`, etc.) resolves directly on the live sheet at `https://recognitionphysics.org/map/#<ID>`, linking this print architecture permanently to the interactive derivation atlas.

8.3 Concluding perspective: what knowing the whole shape changes

When science is pursued piecemeal, open questions look like invitations to invent a new field, a new particle, or a new free parameter. Inside one rigid shape, that escape hatch closes. Knowing all fifteen domains at once reveals that the log-space reciprocal-conductance mirror $\rho = I - \frac{1}{2}\mathbf{1}\mathbf{1}^\top$ of Einstein–Hilbert gravity is the exact extra F_4 symmetry mirror of the D_4 double-entry cell that kills fourth-order anisotropy across matter, gauge plaquettes, and bond-local gravity simultaneously; that every bond's eight triangular continuations form a 3D cube graph-isomorphic to Q_3 carrying the eight-tick Gray clock as a Hamiltonian cycle and yielding the exact trace-free continuum Maxwell stress on one finite cell when weighted by

both rebuilt bond conductances; that the empty balanced ledger carries zero energy and zero volume-current gravitational source; and that 4,095 physical facts (96.1%) compress into one seven-law core and eleven master trunks while isolating the remaining 166 open statements onto eleven sharp, constructive targets. The map is no longer a wish list of unifications—it is a single geometric object whose derived interior passes its checks cleanly and whose outer boundary names every remaining obligation.

A The Complete 15-Domain `/map` Atlas and Print Micro-Sheet

Table 9 records the exact domain-by-domain and level-by-level audit of all 4,261 named statements on `recognitionphysics.org/map/` as of 26 November 2026 (2:23 PM CT), generated directly from the live `sheet.json` snapshot and cross-indexed against the canonical `FirstLedger v2.2.6` archive (21,978 Lean files, 326,434 theorems) and pinned non-biological baseline index (`MAP_INDEX`, 3,157/3,273 Lean-linked = 96.46%, plus newly promoted `R-0067`). Domains `B` and `X` are tabulated strictly at structural and status-count scope.

Table 9. Exact 15-domain audit of `recognitionphysics.org/map/` (26 November 2026, 2:23 PM CT). Ink = Unconditional (`Der.`) + Core/Bridge (`Cond.`); Open = Partial + Unstarted.

Code	Domain	Total	Der.	Cond.	Ink	Open	Ink %	Reb.
F	Foundations and mathematics	251	149	99	248	3	98.8%	84
S	Space, time and relativity	165	5	158	163	2	98.8%	143
Q	Quantum mechanics	264	25	239	264	0	100.0%	225
E	Fields and forces	260	7	244	251	9	96.5%	230
P	Particles and nuclei	295	1	210	211	84	71.5%	185
A	Atoms	302	5	296	301	1	99.7%	284
C	Molecules and chemistry	383	2	381	383	0	100.0%	364
M	Condensed matter	593	20	569	589	4	99.3%	535
T	Heat and statistical physics	280	9	269	278	2	99.3%	251
U	Fluids, materials and surfaces	231	0	231	231	0	100.0%	217
L	Light and radiation	164	2	161	163	1	99.4%	158
G	Gravity, astrophysics and cosmology	285	3	245	248	37	87.0%	224
B	Life: biomolecules[†]	447	0	447	447	0	100.0%	217
X	Life: cells and organisms[†]	225	2	223	225	0	100.0%	205
R	Recognition boundaries	116	2	91	93	23	80.2%	0
All	**15 domains (13 public non-bio + 2 status-only)**	**4,261**	**232**	**3,863**	**4,095**	**166**	**96.1%**	**3,322**

[†]Domains B (447) and X (225) appear strictly as structural status counts; proprietary biomolecular folding, hydration, and binding laws are withheld from public disclosure.



Figure 7. Complete 15-domain print atlas of `/map`. Vector micro-typography specimen generated directly from `sheet.json` (26 November 2026, 2:23 PM CT; `FirstLedger v2.2.6`), displaying all 3,589 public non-biological statements across thirteen domains and five depth levels in solid ink (3,423) and open frontier frames (166), together with aggregate structural status-count blocks for domains `B` (447) and `X` (225; total 4,095 in ink, 4,261 overall).

Table 10. Stratification of all 4,261 map statements by hierarchical derivation depth (Level 1 foundational to Level 5 composite).

Depth Level	Total	Ink	Open	Ink Share
Level 1	439	433	6	98.6%
Level 2	978	947	31	96.8%
Level 3	1,409	1,380	29	97.9%
Level 4	993	921	72	92.7%
Level 5	442	414	28	93.7%
Total	**4,261**	**4,095**	**166**	**96.1%**

References

[1] J. Washburn and M. Zlatanović, "Uniqueness of the canonical reciprocal cost," *Mathematics* **14**(6), 935 (2026), doi:10.3390/math14060935.

[2] S. Pardo-Guerra and J. Washburn, "Three dimensions from a recognition requirement," *Entropy* **28**(11), 1256 (2026).

[3] J. Washburn, "The law of motion on the recognition ledger," Recognition Physics Institute monograph (2026), https://recognitionphysics.org/publications/law-of-motion/LawOfMotion.pdf.

[4] J. Washburn, "The mass table from the recognition ledger (v1.5)," Recognition Physics Institute monograph (2026), https://recognitionphysics.org/publications/the-mass-table/TheMassTable.pdf.

[5] J. Washburn, "The fine-structure constant from the recognition ledger (v1.9.2)," Recognition Physics Institute monograph (2026), https://recognitionphysics.org/publications/fine-structure-constant/FineStructureFromTheLedger.pdf.

[6] J. Washburn, "Quantum gravity from the recognition ledger (v5.0)," Recognition Physics Institute monograph (2026), https://recognitionphysics.org/publications/quantum-gravity-from-the-recognition-ledger/QuantumGravityRecognitionLedger.pdf.

[7] J. Washburn, "Machine-verified Kerr–Newman horizons, nonsingular gravitational collapse, and quantum horizon obstructions," Zenodo archive doi:10.5281/zenodo.24513292 (2026).

[8] J. Washburn, "Black hole evaporation, Page-curve remnants, Lorentzian spin-foam vertices, and rotating nonsingular bounce cores," Zenodo archive doi:10.5281/zenodo.24541030 (2026).

[9] M. Simons, J. Washburn, and E. Allahyarov, "Binary marginal invariance and the quadratic probability rule," *Quantum Studies: Mathematics and Foundations* (accepted, 2026).

[10] Recognition Physics Institute, “The Map of Reality: Live Derivation Ledger,” `https://recognitionphysics.org/map/` (snapshot 26 November 2026, 2:23 PM CT; `FirstLedger v2.2.6`; SHA-256 `8cff5581e034...fddb855e0`).

[11] J. Aczél, *Lectures on Functional Equations and Their Applications*, Academic Press, New York (1966).

[12] J. Lamperti, “On the isometries of certain function-spaces,” *Pacific Journal of Mathematics* **8**(3), 459–466 (1958).

[13] M. B. Hastings, “An area law for one-dimensional quantum systems,” *Journal of Statistical Mechanics* P08024 (2007).

[14] R. N. Hill, “Proof that the H^- ion has only one bound state,” *Physical Review Letters* **38**, 643–646 (1977).

[15] H. Neuberger, “Exactly massless quarks on the lattice,” *Physics Letters B* **417**, 141–144 (1998).

[16] G. Bressi, G. Carugno, R. Onofrio, and G. Ruoso, “Measurement of the Casimir force between parallel metallic surfaces,” *Physical Review Letters* **88**, 041804 (2002).

[17] G. Caldwell and P. Kebarle, “Binding energies and structural effects in halide anion–ROH and −RCOOH complexes from gas-phase equilibria measurements,” *Canadian Journal of Chemistry* **63**, 1399–1406 (1985).

[18] Planck Collaboration, “Planck 2018 results. VI. Cosmological parameters,” *Astronomy & Astrophysics* **641**, A6 (2020).

[19] M. Tristram *et al.*, “Improved limits on the tensor-to-scalar ratio using BICEP and Planck data,” *Physical Review D* **105**, 083524 (2022).

[20] DESI Collaboration, “DESI DR2 results II: Measurements of baryon acoustic oscillations and cosmological constraints,” `arXiv:2503.14738` (2025).

[21] F. Takahashi *et al.* (Particle Data Group), “Review of Particle Physics,” *International Journal of Modern Physics A* **41**, 2630011 (2026).

[22] Direct lattice-QCD determination of the hadronic running of α_{em} ($\Delta\alpha^{(5)}_{\mathrm{had}} = 0.027821(34)(35)$), `arXiv:2607.03370` (2026).

[23] W. Russell, *The Universal One*, Brieger Press, New York (1926).